Sustainable Carbonized Biomass-stabilized Phase Change Materials for Thermal Energy Storage

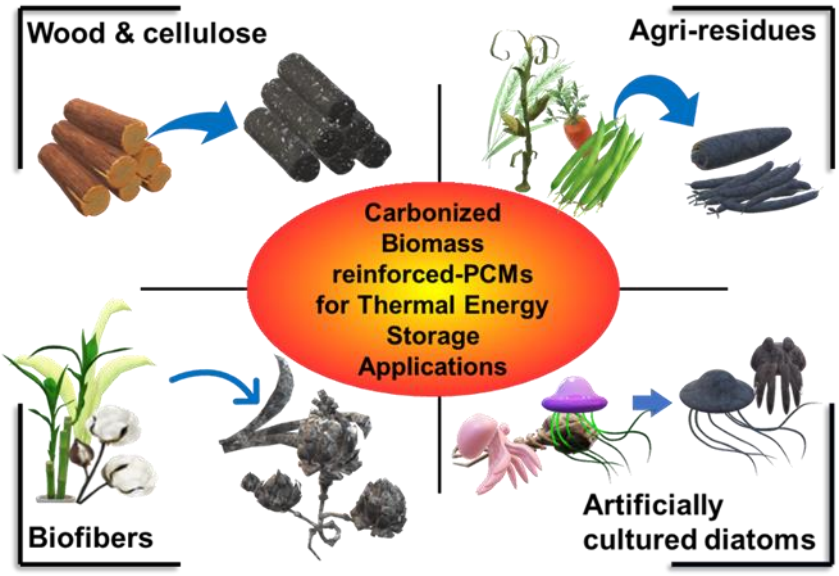
Joseph Kinyanjui Muiruri,[a§] Alvaro Castillo Bonillo,[b,c§] Mingsheng Zhang,[b§] Pengyu Wang,[d,f§] Nikodem Tomczak,[b] Wenya Wu,[b] Xikui Zhang,[b] Suxi Wang,[b] Warintorn Thitsartarn, [b] Pin Jin Ong,[b] Jayven Chee Chuan Yeo,[b] Jianwei Xu, [a,b,e] Zibiao Li, [a,b] Xian Jun Loh* [b], Qiang Zhu*[b,d]

a. Institute of Sustainability for Chemicals, Energy and Environment (ISCE2), Agency for Science, Technology and Research (A*STAR), 1 Pesek Road, Jurong Island, Singapore, 627833, Republic of Singapore
b. Institute of Materials Research and Engineering (IMRE), Agency for Science, Technology and Research (A*STAR), 2 Fusionopolis Way, Innovis #08-03, Singapore 138634, Republic of Singapore
c. Department of Chemistry, Christopher Ingold Building, University College London (UCL), 20 Gordon Street, London, WC1H 0AJ, UK
d. School of Chemistry, Chemical Engineering and Biotechnology, Nanyang Technological University (NTU), 62 Nanyang Drive, Singapore 637459, Republic of Singapore
e. Department of Chemistry, National University of Singapore, 3 Science Drive 3, Singapore 117543, Republic of Singapore
f. Guangdong Midea Air Conditioning Equipment Co., Ltd., No. 22, Lingang Road, Beijiao, Shunde, Foshan, Guangdong, China.

[§] The authors contribute equally to this manuscript.

Corresponding email address: lohxj@imre.a-star.edu.sg; zhuq@imre.a-star.edu.sg

Graphical Abstract



Abstract

Phase change materials (PCMs) integrated with stabilizers from carbonized natural and artificial biomaterials present significant opportunities for thermal energy storage. Natural materials like wood-derived, cellulose-derived, and biofiber carbon reinforcements offer sustainable, cost-effective solutions with benefits such as high surface area, tailored porosity, and improved thermal conductivity. These reinforcements also support waste valorization and environmental sustainability. Artificial biomaterials, on the other hand, provide tunable properties and advanced functionalities. This review covers recent advancements in PCMs stabilized by both natural (including agricultural residues) and artificial biomaterials, highlighting their applications in building insulation, electronics cooling, and transportation temperature regulation. We conclude by giving insights, highlighting gaps, and future directions into the potential for these materials to create sustainable, efficient solutions across various sectors.

Keywords: Phase Change Materials, Stabilizers, Carbonized Materials, Artificial Biomaterials, Thermal Energy Storage

Table of Contents

1. Introduction....4
2. Natural materials-stabilized phase change materials....7
2.1 Wood-Derived Carbon Reinforcements....7
2.2 Cellulose-Derived Carbon Reinforcements....23
2.3 Biofibre Carbon Reinforcements....30
2.4 Agricultural residues-Derived Carbon Reinforcements....32
3. Artificial biomaterials-stabilized phase change materials....38
4. Applications of sustainable carbonized biomass-stabilized PCMs....41
5. Challenges, Existing research gaps and Future directions....49
5.1 Challenges in the real applications of PCM-integrated building designs/systems....49
5.2 Fire prevention technology in reinforced composite PCMs....49
5.3 Existing research gaps and Future directions....50
6. Conclusion....50

1. Introduction

As the world population grows and economies develop, the global energy demand rises [1, 2]. Traditional energy sources, predominantly fossil fuels, are finite and detrimental to the environment, highlighting the urgency for alternative energy solutions [3]. Renewable energy sources like solar and wind offer promising alternatives, but their intermittent nature requires effective energy storage solutions to ensure reliable supply and grid stability [4-6]. Therefore, meeting this energy demand sustainably and efficiently poses significant challenges, necessitating innovative solutions in energy storage technologies [7, 8]. Notably, the best methods for preserving energy and safeguarding the environment are using renewable resources and advancing energy storage technologies [9-14].

Energy storage systems play a fundamental role in balancing supply and demand, smoothing out fluctuations, and integrating renewable energy sources into the grid [15]. In this regard, phase change materials (PCMs) have emerged as a promising option for latent heat thermal energy storage (LHTES) due to their high energy density and ability to store and release thermal energy during phase transitions [16, 17]. However, traditional PCMs suffer from leakage, phase

separation, and low thermal conductivity, limiting their practicality and efficiency. Leakage poses environmental risks and compromises the longevity of PCM-based systems [18]. To address these challenges, form-stable PCMs (FSPCMs) have been developed by incorporating PCM into reinforcements, enhancing structural integrity and thermal properties while minimizing leakage [19, 20]. Natural-derived reinforcements such as cellulose [21, 22], lignin [23], and other natural fibers are abundant, renewable, and biodegradable, making them environmentally friendly alternatives to synthetic supports [24-26]. These reinforcements improve the mechanical strength and thermal conductivity of PCMs, enhancing their stability and overall performance [27, 28]. Additionally, natural-derived reinforcements exhibit good compatibility with PCMs, ensuring homogeneity and uniform distribution within the composite material [29, 30].

The performance of PCMs largely depends on the matrix they are embedded in, and porous carbon-based materials have emerged as promising matrix supports.[31] The representative examples include graphene, graphene oxide (GO), and carbon nanotubes (CNTs). [31, 32] Graphene and derivatives strengthen the PCM in terms of higher heat transfer rates due to their higher thermal conductivity and mechanical strength.[33] Unfortunately, their high production cost,environmental effect, and scalability issues restrict their wide application. CNTs provide very good thermal and electrical conductivity with strong mechanical strength and, therefore, are considered suitable for high-performance PCMs.[34] However, the synthesis of CNTs is costly and involves health hazards; thus, it may not be practical compared to other low-cost materials such as carbonized biomass. Activated carbon is another widely used matrix for PCMs, valued for its high surface area and porosity, which provide effective thermal management and stability.[8] Although it is generally more cost-effective than graphene and CNTs, it can still be pricier than carbonized biomass when factoring in the costs of activation processes. Highly porous and low-density carbon aerogels are especially good for thermal insulation and energy storage.[35] Complex and expensive manufacturing processes limit the applications of carbon aerogels to only some specialized areas.[36] Readers can also refer to a recent reviews on porous carbon materials for comprehensive understanding of these materials in phase change applications.[37-42]

Carbonized biomass presents a compelling alternative to other carbon-based porous materials in the context of PCMs and represents a significant advancement in PCM technology, offering tailored solutions with superior properties [31, 43, 44]. Through controlled pyrolysis processes, natural materials such as biomass and agricultural waste can be transformed into carbonized

structures with enhanced mechanical strength, thermal conductivity, and stability [8, 45, 46]. Carbonized reinforcements exhibit improved resistance to degradation and phase separation, addressing key challenges associated with traditional PCMs [47, 48]. Furthermore, the carbonization process allows for the customization of properties, enabling optimization for specific applications and operating conditions [49]. Carbonized materials are superior to non-carbonized counterparts as PCM supports or reinforcements due to their high thermal conductivity, thermal stability, mechanical strength, chemical inertness, and environmental sustainability [50]. Song's group [51] developed a biomass-derived carbon scaffold from a loofah sponge. The resultant scaffold exhibited a large specific surface area (668.75 m^2/g) and micropore area (303.37 m^2/g), preventing poly(ethylene glycol) (PEG) leakage while providing thermal and electrical conductivity. The PCM showed a high TES density (137.6 J/g), superior electric-to-thermal conversion, and enhanced thermal resistance. On the other hand, uncarbonized loofah sponge-PCM material depicted 99.2 J/g, which is ~39% less compared with its carbonized counterpart. Therefore, the properties of carbonized materials enable efficient heat transfer during phase change processes, enhancing the thermal performance of PCM-based systems [52].

Carbonized materials also maintain structural integrity across a wide temperature range, preventing degradation in PCM applications [53]. They also have superior mechanical strength, ensuring PCM encapsulation remains intact under mechanical stresses, preventing leakage or structural failure [54-56]. For instance, Luo *et al.* [54] designed a shape-stabilized PCM (SSPCM) using activated garlic peel and paraffin via vacuum impregnation. Activated garlic peel was found to have numerous grooves and pores, with a high specific surface area of 1309 m^2/g. The resulting PCM exhibited excellent shape stability, thermal stability, and waste heat storage capacity. Moreover, it showed a low latent heat loss rate of about 1.5% after 200 thermal cycles. Carbonized materials are chemically inert, reducing the risk of chemical reactions or compatibility issues affecting PCM stability or performance [34]. Additionally, carbonized materials are derived from renewable biomass sources, aligning with sustainability goals by promoting renewable resources and reducing reliance on fossil fuels [57]. Overall, carbonized materials are a preferred choice for PCM supports and reinforcements due to their enhanced thermal performance, durability, and reliability [58].

In addition, artificial PCM reinforcement materials such as artificial cultured diatoms and microscopic algae with elaborate silica shells have found considerable interest in recent years [59-61]. These diatoms are typically cultivated in controlled environments and offer unique

geometric structures and high surface area, suitable for enhancing PCM performance [62]. By integrating carbonized diatom-based reinforcements into PCM matrices, new materials that are lightweight, porous in nature, and thermal stable have been developed [63-67].

Despite growing interest in biomass-derived materials for supporting phase change materials (PCMs) and the availability of numerous reviews on functionalized PCMs (FSPCMs), there is a significant gap in reviews specifically focused on carbonized natural materials as PCM supports. Current literature often overlooks these sustainable materials, concentrating instead on unsustainable carbon sources or specific applications.[25, 68-70] Addressing this gap is essential, as carbonized natural materials have the potential to enhance PCM performance while supporting environmental and economic goals. A thorough evaluation of these materials would provide crucial insights into their benefits and challenges, promoting more sustainable and effective PCM solutions. This current review is essential, as it presents a close view of recent developments in natural material-stabilized PCMs, including wood, cellulose, biofibers, agricultural residues, and artificial biomaterials. It explores how these innovative materials are applied in critical areas such as building insulation, electronics cooling, and temperature regulation in transportation systems. Importantly, it covers the current challenges, identifies existing research gaps, and outlines future development directions. By highlighting these aspects, the review emphasizes the potential of these materials for delivering sustainable and efficient energy storage solutions. It offers valuable insights for overcoming obstacles and guiding future research efforts.

2. Natural materials-stabilized phase change materials

2.1 Wood-Derived Carbon Reinforcements

To reduce carbon emissions, various sustainable materials and technologies have been widely studied [71-77]. Wood, a porous, fibrous lignocellulosic material found in tree stems and roots, supports plant structure and facilitates nutrient and water movement [78-80]. Its primary constituents include cellulose, hemicellulose, and lignin, as depicted in Figure 1 [80]. Wood is a sustainable, renewable resource for building, furniture, and paper manufacturing. As shown in Figures 1a, c, balsa, and cork wood feature abundant anisotropic pores with a diverse size distribution. For instance, balsa depicts the presence of vessels of maximum pore size of 23.15μm, while the fiber structure appears entangled, resulting in a dense image via scanning electron microscopy (SEM) analysis, as shown in Figure 1(b1). On the other hand, cork reveals

a porous internal structure characterized by a multitude of pores and a honeycomb-like arrangement. The pore sizes in cork range from 19.76 to 49.76 µm, as shown in Figure 1(b2).

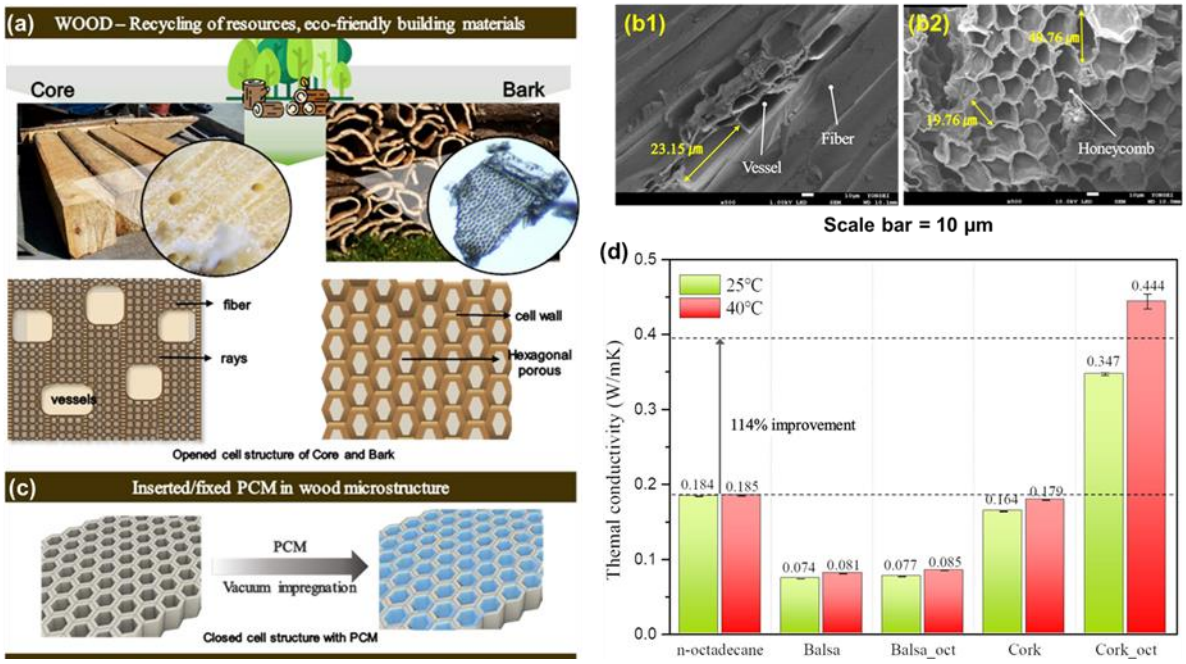


Fig. 1. (a) Schematic representation of wood (bark, core) structure, (b1,b2) SEM images of balsa and cork, respectively, (c) impregnation process of porous wood structure with PCM, and (d) thermal conductivity values at different temperatures. Reproduced with permission from [80]. Copyright (2022), John Wiley and Sons.

Despite wood's low thermal conductivity, its vertically oriented and ordered pore structure offers a clear pathway for mass and energy transmission [81, 82]. These distinctive characteristics render wood highly suitable for applications in PCMs for energy storage purposes, particularly as a supportive material [83-85]. A straightforward method of utilizing wood as support materials for energy storage involves immersing the wood into a liquid PCM, allowing the PCM to impregnate the wood pores, as illustrated in Figure 1c. Typically, this impregnation process takes place within a vacuum system to enhance impregnation efficiency. After impregnating balsa and cork wood with n-octadecane, Nam *et al*. [80] reported that thermal conductivity values for SSPCMs, Balsa_oct and Cork_oct were greater than n-octadecane. It is worth noting that Cork_oct's thermal conductivity increased by 114% compared to n-octadecane due to more pores in the porous material (Figure 1d). Heat conduction and fluid convection occur more quickly and intensely in cork due to stored heat, affecting heat conductivity and PCM's ability to accumulate heat [86]. Moreover, results

indicated that Balsa_oct exhibited an average heat storage capacity of 49.65 J/g, whereas Cork_oct demonstrated an average latent heat capacity of 131.21 J/g. However, during heating, PCM leakage was observed in Balsa_oct after 2 h at approximately 50 °C, while Cork_oct experienced gradual PCM leakage over 4 h.

In another study, Saavedra *et al*. [87] utilized *Pinus radiata* wood impregnated with octadecane via a double vacuum method to produce an SSPCM. Their investigation revealed that the PCM impregnation did not significantly alter the mechanical properties of the wood, including Young's modulus and maximum stress. These results suggest that PCM-infused wood holds potential for various applications in building construction, including use in walls, floors, beams, and columns. However, it is imperative to coat the wood to prevent the leakage of octadecane during solid-liquid phase transitions. Fuentes-Sepúlveda's team [88] investigated the effective heat storage capacity of octadecane in conjunction with the construction and production potential of *Pinus radiata*. Differential scanning calorimetry (DSC) analysis revealed that the composite material exhibited fusion enthalpy values ranging from 36 J/g to 122 J/g. Utilizing the transient line heat source method, the study demonstrated that impregnating *Pinus radiata* with octadecane enhanced its specific heat within the temperature range of 15 to 20 °C. Interestingly, the thermal conductivity of the wood decreased in the radial and tangential directions while increasing in the longitudinal direction.

Liang *et al*. [89] developed SSPCMs using PEG/wood flour (WF) composites as depicted in Figure 2a. These SSPCMs, with varying average molecular weights of PEG and different length-to-diameter ratios of WF, were prepared through a simple vacuum adsorption process. They observed that WF with a high length-to-diameter ratio (HWF) exhibited significantly higher adsorption capacity for PEG compared to WF with a low length-to-diameter ratio (LWF).

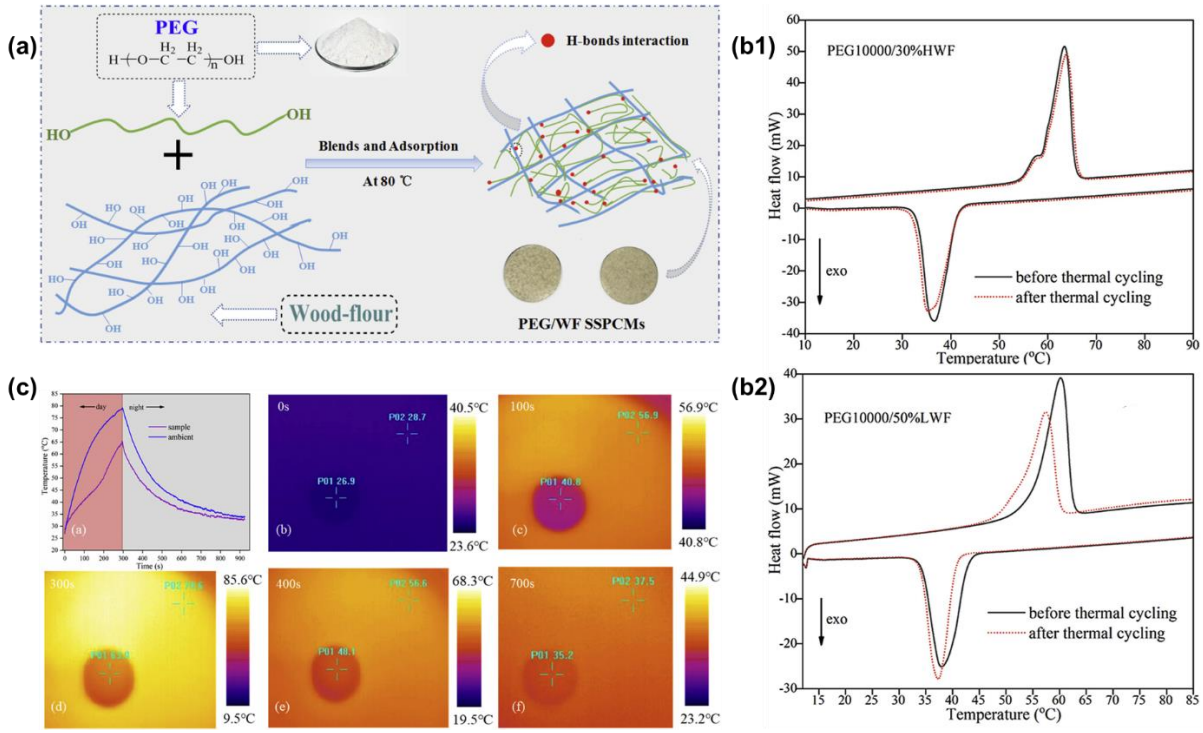


Fig 2. (a) synthetic route of PEG/WFSSPCMs, (b1, b2) DSC graphs of SSPCMs before and after thermal cycling, and (c) Temperature-time profiles of the sample and its surrounding environment, along with illustrative thermal images displaying photothermal performance. Reproduced with permission from [89] Copyright (2019), Elsevier.

PEG/HWF composites show excellent shape stability and adsorption content, with a maximum of 70 wt% PEG content. PEG1000/HWF SSPCMs have a maximum PEG content of 75 wt% without leakage above the melting point, and the highest melting latent heat is 108.6 J/g. Maintaining thermal stability and reusability are vital for PCMs. DSC results show PEG10000/HWF are thermally stable, with comparable melting and crystallization temperatures in both cycles, as depicted in Figures 2b1, b2. Additionally, evaluated tests of light-to-thermal conversion and temperature adjustment capabilities using an infrared thermography camera were done, and the temperature-time curves and environment evolution are shown in Figure 2c. As shown, a cylindrical sample and its environment, denoted as P01 and P02, respectively, the sample's temperature initially mirrors the ambient temperature, resulting in a blue image. However, with solar irradiation, the temperature increases rapidly, causing the image to shift towards red. This makes the sample suitable for cool energy storage systems in buildings with ambient temperatures between 30 and 45 °C [83, 89-92].

In an interesting work, Zhao *et al*. [93] explored wood-plastic composites (WPCs) as another wood-based PCM, employing wood fiber/high-density polyethylene as the matrix and PEG/organic diatomite (O-Dt) PCM as the phase change heat storage medium. Their study researched the thermal and mechanical properties of these heat-storage WPCs with varying weight fractions of FSPCMs. The investigation revealed that organic modification in PCM with PEG/O-Dt facilitated better encapsulation of PEG compared to PCM with PEG/Dt. The thermal enthalpy of PCM with PEG/O-Dt reached 105.35 J/g, with a supercooling degree of 0.46 °C. These heat-storage WPCs exhibited commendable temperature-regulating ability, with an enthalpy value reaching 60.42 J/g. After 500 cycles, the thermal reliability and stability of the heat storage WPCs remained robust. The highest heat conduction of the WPCs reached 0.28 W/(m·K), signifying significant enhancement. Moreover, the mechanical properties and hydrophobicity of the heat storage WPCs were also improved owing to the incorporation of PEG/O-Dt.

Ma's group [94] explored the delignification treatment of wood, which involves the removal of full or partial lignin while preserving its hierarchically aligned cellulosic structure—a conducive environment for PCM storage. In their study, delignified wood (DW) was prepared through chemical treatment with a solution of NaOH (2.5 mol/L) and Na_2SO_3 (0.4 mol/L), followed by boiling for 12 h to remove lignin. Initially, the wood exhibited a porous honeycomb-like structure with organized cell walls sporting thick and smooth surfaces. After delignification, the porous honeycomb-like structure of the DW remained intact, albeit with thinner cell walls and enlarged pores. Notably, microscale pores emerged within the cell walls, facilitated by lignin removal. Removing lignin and associated pore-blocking substances led to unobstructed tube-like cells and cell cavities, which were advantageous for adsorption. This structural modification enhanced the interaction between DW and the PCM in DW/capric acid-palmitic acid (CA-PA) FSPCM compared to wood/CA-PA FSPCM. Particularly, strong hydrogen bonds facilitated the filling of most pores within DW/CA-PA FSPCM, while only partial pores of wood/CA-PA FSPCM were filled. These observations highlight the effectiveness of delignification in enhancing PCM adsorption within wood structures, particularly in DW configurations.

In another work, Sun *et al*. [95] studied removed lignin from platane wood and subsequently prepared a series of FSPCMs using the vacuum impregnation method. The fatty acids used for impregnation included dodecanoic (lauric) acid (LA), tetradecanoic (myristic) acid (MA), PA, and octadecanoic (stearic) acid (SA). Their research demonstrated that DW exhibited excellent

support for PCM. The impregnation rates of LA, MA, PA, and SA in DW were notably higher than untreated wood, reaching 79.7%, 78.1%, 76.1%, and 77.9%, respectively. Moreover, the entrapment efficiencies of DW/LA, DW/MA, DW/PA, and DW/SA FSPCMs were notably boosted, with enhancements of 18.1%, 15.5%, 20.4%, and 22.5%, respectively, compared to their wood counterparts. Fourier transform infrared spectroscopy (FTIR) and X-ray diffraction (XRD) analyses revealed solely physical interactions between DW and fatty acids. Particularly, XRD findings illustrated DW's ability to inhibit LA crystallization. Moreover, the melting and solidification phase change temperatures of DW/LA experienced insignificant changes after 500 thermal cycles. Similarly, the melting and solidification latent heat of DW/LA decreased by 2.5% and 2.0%, respectively. These findings accentuate the potential of DW as an effective matrix for FSPCMs systems, highlighting its capability to enhance impregnation rates and entrapment efficiencies while maintaining thermal stability over repeated thermal cycles.

To address the issues of liquid leakage post-phase shift and insufficient heat conductivity of PCMs, which are impeding their application, various solutions have been pursued [42, 96-98]. Chen *et al*. [81] investigated delignified balsa wood (WOOD)-based PEG composite with varying proportions of boron nitride (BN) filler. Upon penetration of PEG6000 into delignified balsa wood, the crystallinity increased due to the restriction of pore size and external negative pressure, prompting a more orderly stacking of molecular chains. The melting and freezing enthalpies of WOOD/PEG6000 were found to be 209.3 J/g and 214.9 J/g, respectively, enhancement of 7.2% and 7.3% compared to pure PEG6000. Additionally, the extrapolated decomposition temperature of WOOD/PEG6000 (381 °C) surpassed that of PEG6000 (342 °C) or WOOD (314 °C). Furthermore, the thermal conductivity improved compared to WOOD/PEG6000 upon adding BN into the PCM. For instance, the highest out-of-plane thermal conductivity, reaching 0.96 W/(m·K) with 33 wt% BN, was approximately three times higher than that in the radial direction (0.36 W/(m·K)). Potential uses for this adjustable anisotropic thermal conductivity could be found where forced unidirectional heat dissipation is necessary. Moreover, the study revealed that the PCM composite transitioned from a typical rigid solid material to one with excellent bending and compression properties upon heating beyond the phase transition temperature.

Meng *et al*. [99] engineered balsa-based FSPCMs through selective lignin removal. Figure 3 shows the morphology and cross-section of untreated balsa wood, scaffolds from DW (W-L), and DW after hemicellulose removal (W-L, H), and FSPCMs post-PEG loading. In Figure 3a1, balsa wood has a pale-yellow hue due to lignin chromophores and the resulting morphology in

Figures 3a2, a3. Post-delignification, chromophore groups vanish, resulting in a white scaffold with reduced cell wall thickness and vertically aligned vascular structures and microstructure in Figures 3b1, b3, respectively. The removal of hemicellulose in Figure 3c1 significantly impacts the morphology of W-L in Figures 3c2, c3. Furthermore, in Figures 3d-f, the FSPCM composite material showed a seamless integration of PEG in macro-scale vascular pores, indicating a strong affinity between PEG and scaffold walls. The removal of lignin and hemicellulose enhanced the permeability of the composite PCMs (CPCMs), while hemicellulose provided compressive resistance. The CPCMs had high porosity, low density, superior mechanical properties, high encapsulation capability, and exceptional dimensional stability. The FSPCM showed desirable phase transition temperatures with melting and crystallization points of 40.0 °C and 27.7 °C, respectively, and corresponding latent heat of 134.3 J/g and 125.3 J/g. The FSPCM based on delignified balsa wood showed no degradation of latent heat or fluctuation in phase transition temperature over 200 continuous heating/cooling cycles. The FSPCM also demonstrated prolonged durations for TES and release during heating and cooling processes, shown in Figure 3g, compared to the pristine DW scaffold without encapsulated PEG. Notably, untreated wood contains lignin that fills cellulose microfibrils, reducing effective adsorption sites (-OH) on cellulosic surfaces to hydrogen bond with PEG via proposed interactions in Figure 3h.

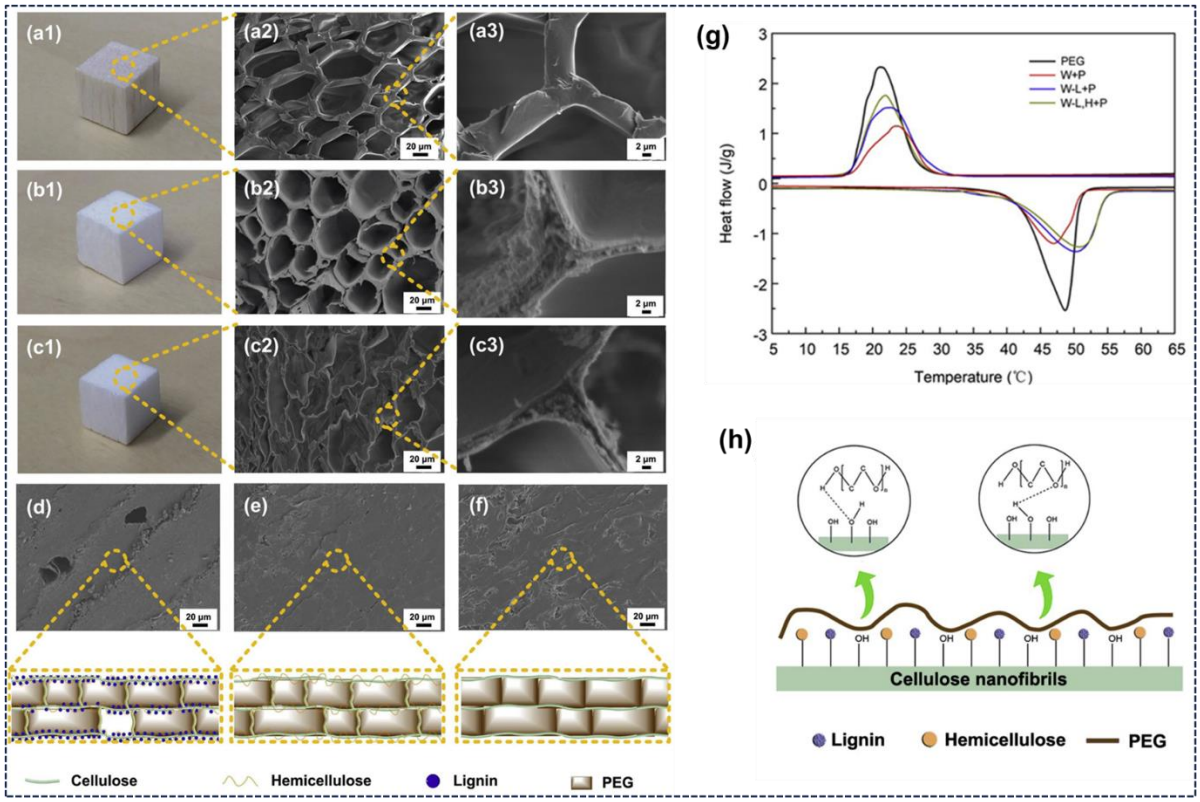


Fig. 3. Photographs of untreated balsa wood, W(a1), W-L(b1), and (c1) W-L & H and their SEM cross-section images at low and high resolution (a2, a3, b2, b3, c2, and c3). Axial section morphology was obtained from untreated balsa (d) W + PEG, (e) W-L + PEG, and (f) W-L, H + PEG. (g) DSC curves of PEG, W + PEG, W-L + PEG, W-L, H + PEG and (h) Schematic illustrations of the proposed interactions between PEG and the FPCM scaffolds in W + PEG. Reproduced with permission from [99] Copyright (2020), Elsevier.

In another work [100] using a cellulose matrix, the co-precipitation method was used to merge Fe_3O_4 nanoparticles into PCMs, enhancing their efficiency in converting light into thermal energy. The layered cellulose skeleton allows superior encapsulation, resulting in CPCMs with unmatched thermal reliability and self-cleaning capabilities. To illustrate, adding 0.05 and 0.5% Fe_3O_4 nanoparticles to CPCMs increases thermal conductivity from 0.28 W/(m·K) to 0.41 W/(m·K), respectively. This increment is equivalent to 12–64% of pure PEG. Additionally, the CPCMs maintain a high latent heat of 172.6–177.7 J/g and improve light absorption capacity and conversion efficiency by roughly 71–87%. This approach results in high latent heat and energy-efficient solutions in material science, demonstrating the potential for intelligent building thermal regulation and a sustainable strategy for producing leak-free CPCMs.

Carbonized wood (CW) represents a state where the cellular structure of wood is retained, offering a high solar light absorption rate. For instance, Pan *et al*. [101] studied the treatment of balsa wood through delignification and carbonization to achieve a regular pore structure, allowing for the impregnation of PCM (OP44E) to form CW/OP44E CPCMs. The study found that CWs retained a porous structure like balsa wood, with a porosity of up to 92.03%. The maximum effective impregnation ratio of PCMs into CW-3 was 85.25 wt%. The photo-thermal conversion efficiency of the CPCM reached 90%, with a decrease of less than 10% after 30 cycles. In a similar work, Li *et al*. [102] used CW loaded with carbon dots (CDs) as a supporting material for PEG to create an SSPCM. The resultant PCMs showed abundant pore structures in both CW and CW-CDs, maintaining natural wood's straight channels. Upon loading PEG, CW-PEG and CW-CDs-PEG displayed smoother surface morphology. The porous structure of CW-CDs, combined with the surface polarity functional groups of CDs, enhanced resistance to PEG leakage during heating. The interconnected carbon skeleton of CW also improved thermal conductivity, enhancing the CPCMs' efficiency. The porous structure of CW-CDs and surface polarity functional groups enhance resistance to PEG leakage during heating. The interconnected carbon skeleton enhances thermal conductivity, enhancing the performance of CPCMs. The CPCM has a remarkable 117% increase in thermal conductivity (0.449 W/(m·K)) compared to pure PEG, efficient photo-thermal conversion at 84.4%, substantial energy storage capacity (112.4 J/g), and good thermal reliability even after 50 heating-cooling cycles.

Wan’s team [103] developed an FSPCM by utilizing pinecone biochar (PB) as a supporting matrix for polyamide (PA). PB was derived from residual pinecone forest material. The biochar offers affordability, environmental friendliness, and easy preparatory procedures. Then, PA was physically absorbed within the PB structure while maintaining its crystal integrity. PA/PB-4 exhibited fusion and crystallization points at 59.25 °C and 59.13 °C, respectively, accompanied by fusion and freezing latent heat of 84.74 J/g and 83.81 J/g. The thermal stability of the composite was notably high, rendering it well-suited for TES purposes. With a heat conduction of 0.3926 W/(m·K), PA/PB-4 expressed about 44% enhancement compared to pure PA, highlighting its considerable potential for TES applications.

Feng and coworkers [104] developed two high-performance biomass-based shape-stable CPCMs using paulownia chips (DPW) with a retained cellulose skeleton as a structural support. Erythritol, urea (E7U3), erythritol, and thiourea (E7T3) with a mass ratio of 7:3 were used as

the principal PCMs. SEM analysis showed that DPW has a honeycomb-like micropore structure, and E7U3 and E7T3 were effectively loaded into DPW, resulting in high PCM content. These materials exhibit high phase transition enthalpies and remarkable photothermal conversion efficiencies, reaching 72.6% and 75.8%, respectively. FTIR analysis showed no chemical interaction between E7U3 and DPW, suggesting a beneficial physical interaction for leveraging their phase change energy storage characteristics. The study also highlighted the importance of removing non-cellulosic components from cell walls in crafting anisotropic 3D porous scaffolds, which have lower density, increased surface area, and elevated porosity, reaching up to 95%.

To summarize the studies done in this section on wood-based carbon reinforcement materials for PCMs, Table 1 shows the carbon source, PCM matrix, form stabilizer, reinforcement strategy, outstanding properties, purpose, and key findings.

Table 1. Key findings of selected wood-based carbon reinforcement materials and carbon-based porous materials (graphene and derivatives, carbon nanotubes, activated carbon) including carbon source, PCM matrix, form stabilizer, reinforcement strategy, outstanding properties, and purpose.

Carbon source	**Form Stabilizer**	**Reinforcement Preparation**	**PCM**	**Outstanding properties**			**Purpose**	**Key Findings**	**Ref.**
				Melting Temp. (ºC) (Heating/ Cooling)	Latent Heat (J/g) (Heating/ Cooling)	Form-Stability conditions			
Wood Derived Carbon Reinforcements									
Wood	Balsa & cork	• Baking in vacuum • Impregnation in air • Impregnation in Vacuum	n-Octadecane	Balsa_oct: 26.47/23.75 Cork_oct: 27.72/23.40	Balsa_oct: 49.66/49.63 Cork_oct: 131.20/131.22	Balsa_oct: Leaked after 2 h at 50 °C. Cork_oct: Gradual leakage over 4 h.	To enhance wood's heat storage, assess its thermal, morphological, and chemical stability.	1. Balsa_oct has 49.65 J/g heat storage; Cork_oct has 131.21 J/g latent heat. Cork_oct's thermal conductivity increased by 114%, aiding heat transfer. 2. SSPCM thermal stability tested: Balsa_oct leaked after 2 h at 50 °C; Cork_oct leaked gradually over 4 h.	[80]
Wood	Pinus radiata wood	• Impregnation • Hardening epoxy resin coating	Octadecane	15-20 °C	36-122	Epoxy resin coating prevents percolation in impregnated wood above PCM melting temperature	To study the thermal properties of Pinus radiata wood after vacuum impregnation with octadecane	1. Composite material's fusion enthalpy varies from 36 to 122 J/g. 2. Impregnating Pinus radiata with octadecane raises its specific heat at 15-20 °C. 3. Thermal conductivity decreases radially and tangentially but increases longitudinally. 4. Impregnated wood shows phase change enthalpies ranging from 23.8% to 49.9% of octadecane's melting enthalpy in different directions.	[88]

Wood	WF	• Melting • Stirring • Vacuum drying	PEG	45.8-62.8/22.2-39.6	88.9-189.2/77.3-162.7	Phase transition and latent heat of PEG/HWF and PEG/LWF SSPCMs stable after 100 cycles. Chemical structure unaffected by thermal cycling, no degradation observed.	To study the relationship between PEG molecular weight, WF ratio, and PCM properties.	1. High length-to-diameter ratio (HWF) WF showed better PEG adsorption than low ratio (LWF). 2. PEG/HWF PCMs with PEG MW > 4000 have 70 wt% adsorption, with good shape stability. PEG1000 had 75 wt% adsorption without leakage. 3. PEG/HWF SSPCM had 108.6 J/g melting latent heat and >75.05% enthalpy efficiency.	[89]
Wood	Wood fiber	• Stirring • Vacuum drying • Mixing mill • Crushing • Molding • Hot-press • De-molding	Encapsulate PEG/O-Dt	12.74-20.20/26.99-60.42	15.99-16.64/18.73-52.19	After 500 cycles: Melting/freezing temps decreased: -0.99°C, -1.62°C. Latent heat loss: 5.2% (melting), 2.6% (freezing).	To create bio-based heat storage composites: Analyze properties, water absorption, WPC-PCM interaction.	1. PCM2 better: higher enthalpy, lower supercooling. 2. WPCs regulate temperature well; 30% PCM2 maintains high enthalpy. 3. Thermal conductivity peaks at 20% PCM. 4. PEG/O-Dt PCMs enhance WPCs; optimal loading 20% PCM2.	[93]
Wood	DW	• Delignification • Adsorption of CA-PA by vacuum impregnation	CA-PA	23.4/14.5	94.4/91.4	After 100 cycles: Crystallization/melting points: -0.4 °C and +0.2 °C ΔH: -4.3 J/g and +2.1 J/g FTIR: No new bonds, suggesting no degradation.	To make wallboards with fatty acids and wood to store solar heat for day-night release.	1. CA-PA mix infiltrated DW (61.2% ratio), no leaks. 2. SEM: DW has pores filled by CA-PA. 3. FSPCM: 23.4 °C transition, 94.4 J/g latent heat. 4. FSPCM's thermal conductivity rose by 133.3%.	[94]
Cellulose	Platane wood	• Delignification • Adsorption • Dry	LA, MA, PA, and SA	42.16-67.15/40.38-65.80	139.3-166.5/243.7-162.3	DW/LA melting: -0.69%, solidification: +0.20% after 500 cycles. Latent heat: -2.5% (melting), -	To study the potential application of the prepared DW/FA FSPCMs in TES systems.	1. DW prevents LA leakage. 2. Impregnation rates: LA 79.7%, MA 78.1%, PA 76.1%, SA 77.9%. 3. Entrapment efficiencies: DW/LA 82.8%, DW/MA	[95]

						2.0% (solidification).		79.8%, DW/PA 77.4%, DW/SA 78.7%. Increases compared to Wood. 4. FTIR/XRD: Physical interaction between DW and FA. DW restricts LA crystallization. TG: DW/LA FSPCM thermal stability. DW/LA FSPCMs reliable.	
Wood	Wood	• Lye treatment • Hydrogen Peroxide treatment • Vacuum freeze-drying • Vacuum impregnation	PEG6000/BN	N.A.	147.6-190.0/154.3-199.9	After 50 cycles, PCM composite's enthalpy only dropped by 7.5%.	To develop porous wood-based material to encapsulate PCM, enhancing encapsulation rate, energy storage density, anisotropic thermal conductivity, and overall thermal performance.	1. PEG6000 enhances wood crystallinity, increasing enthalpies by 7.2-7.3%. 2. WOOD/PEG6000's higher decomposition temp. (381 °C) surpasses PEG6000 (342 °C) and WOOD (314 °C). BN improves thermal conductivity; max 0.96 W/(m·K) with 33 wt% BN, suitable for unidirectional heat dissipation. 3. CPCM transitions from rigid to flexible upon heating past phase transition temp.	[81]
Wood	Balsa	• Delignification • Treatment of 10 wt% NaOH • Rinsing • Freeze-drying • Vacuum impregnation • Vacuum Drying	PEG 1500	40.0-40.9/27.2-27.7	143.3-135.0/125.3-126.1	After thermal cycling, minimal reduction in melting and cooling latent heat (0.6% and 0.5% respectively). Melting and crystallization temperatures increased slightly (1.5 °C and 1.7 °C respectively).	To develop effective and sustainable 3D porous scaffolds	1. FSPCM made by removing lignin, preserving cellulose, hemicelluloses. 2. FPCM has high encapsulating capacity, 83.5%, latent heat 134 J/g, low supercooling. 3. FPCMs resist compressive loads, stable for 200 heating/cooling cycles, insignificant latent heat loss compared to pure PEG.	[99]

Wood	CW	• Delignification • Freezing drying • Carbonization • Vacuum impregnation • Vacuum drying	OP44E	41.4-41.6/43.29-43.46	201.7-206.3/203.2-210.9	After 30 photo-thermal cycles, enthalpy decreases less than 10%, with CW-1/OP44E (carbonized 1 h at 300 °C) dropping by 4%.	To develop CPCMs for solar energy conversion and efficient energy storage	(1) CWs have high porosity (92.03%), PCMs impregnation ratio up to 85.25 wt%. (2) CW-3/OP44E: phase change temp 41 °C, latent heat 206.3 J/g. (3) CPCMs have a suitable photo-thermal conversion, CW-3/OP44E efficiency 90%.	[101]
Wood	Porous CW loaded with CDs	• Carbonization • Integration with CD • Vacuum impregnation	PEG	51.8/36.5	112.4/100.8	After 50 cycles, Melting Temp: -0.2 °C (Heating), 0.0 °C (Cooling). Latent Heat: +0.4 J/g (Heating), -1.4 J/g (Cooling).	To enhance thermal conductivity and superior photo-thermal conversion efficiency	1. The porous structure of CW-CW-CDs prevent PEG leakage, promote thermal conductivity. 2. PCMs from CW-CDs-PEG show shape stability, high thermal conductivity (0.449 W/(m·K)) (117% higher than that of pure PEG). 3. CW-CDs-PEG: high photo-thermal conversion (84.4%), energy storage (112.4 J/g), thermal reliability & stability (after 50 heating-cooling cycles)	[102]
Wood	Cellulose of paulownia chip	• Delignification (Immersing & dipping) • Washing & freeze-drying • Vacuum impregnation • Freeze-drying	Erythritol-urea and erythritol-thiourea	79.0-120.4	79.82-286.0	After 100 cycles, latent heat remains nearly constant.	To utilize an organic blend of erythritol-urea (thiourea) phase change-antibacterial material and green cellulose-based material for medium-temperature solar and thermal energy harvesting, focusing	1. SEM analysis: DPW has micropore structures. E7U3 and E7T3 loaded into DPW, forming a high PCM load. E7U3-DPW and E7T3-DPW have high phase transition enthalpies. Latent heat remains unchanged after 100 cycles. 2. FTIR analysis: No chemical interaction between E7U3/E7T3 and DPW, only physical interaction. E7U3-	[104]

							on antibacterial and insulation benefits.	DPW and E7T3-DPW have high photothermal conversion efficiencies.	
Porous carbon materials reinforcements									
Multiwalled Carbon nanotube (MWCNT)	-	Acid treatment (H_2SO_4 & HNO_3)	Plusice A70	67.64	159.59	Thermal reliability and chemical stability up to 500 cycles	To investigate thermophysical properties nano dispersed PCM with MWCNT nanoparticles and functionalized MWCNT	1. 1.5-fold thermal conductivity enhancement 2. Homogenous distribution MWCNT in base A70 due to capillary action & surface tension	[105]
MWCNT - oxide	-	Partial unzipping of MWCNTs	PEG	59.81- 60.89	145.49-135.83	Neglible decrease in thermal stability after 100 thermal cycles	To investigate the effect of MCNT-oxide on PEG-based PCM composites properties	1. Thermal conductivity 0.308 W/m-K after 100cycles with 6 wt% MWCNT-oxide addition. 2. Heat transfer rate enhanced by 40 % (heating) and 30 % (reléase).	[106]
Graphene oxide	Graphene oxide aerogels (GA)	hydrothermal method	Paraffin	32.04- 33.24	52.79-53.91	-	To synthesize GA-based paraffin PCC (GAP) & investigate GA's influence on paraffin crystallization and phase change, and predict how GA's pore structure and thermal properties affect GAP's thermal conductivity through finite element simulations	1. Thermal conductivity of sample with 9.2 wt% GA content ~0.81 W/m·K	[107]
Porous Carbon	Carbon fibers	Interlayering carbon fiber (CFRP), EG/Paraffin	Ethylene glycol (EG)	49.3-51.8	16.21-15.08	Less than 9% change in enthalpies after 400 times and 800 times thermal cycles	To prepare unidirectional CFRP-EG/Paraffin composite and study their performance	1. Thermal conductivity of sample ~2.4W/m·K	[108]

Palm kernel shell-activated carbon	Activated carbon	Epoxy resin coating	Paraffin	29.2-31.6	57.3−57.2	After 2000 cycles, thermal stability maintained ~30.2 (melting) & ~32.5 (solidification)	To develop a form-stable composite PCM using oil palm kernel shell-activated carbon & investigate the compressive strength and thermal properties of concrete-reinforced with composite PCM.	1. Compressive strength of Concrete with composite PCM more than 15 MPa after 28 days 2. Good stability against thermal degradation & excellent chemical stability	[109]
Coal-based ultrathin-wall graphitic porous carbon	Graphitic porous carbon	Impregnation method	Paraffin	170.1 - 187.4	-	After 300 cycles, 98% capacity retained	To develop 3D hierarchical porous graphitic carbon from coal	1. Specific surface area ~1351 m^2/g 2. 90 wt% paraffin@GPC melting enthalpy ~ 187.4 $kJ \cdot kg^{-1}$ 3. Thermal conductivity of 0.58 $W \cdot m^{-1} \cdot K^{-1}$	[110]

2.2 Cellulose-Derived Carbon Reinforcements

Nowadays, using natural materials for various applications has attracted more attention [111-114]. Cellulose is an organic compound produced by plants, algae, and certain bacteria, known for its non-toxic, non-allergenic, biodegradable, and renewable nature [115]. It is the primary structural component in plant and algae cell walls, consisting of hundreds to thousands of glucose molecules linked together. The stability of cellulose is due to the dense network of hydrogen. The unique network structure, mechanical properties, and specific surface area of cellulose enable its effective integration through layer-by-layer self-assembly, in-situ chemical polymerization, and electrochemical deposition [116]. These methods allow for the incorporation of various nanoparticles, such as metal oxides, conductive polymers, and 2D nanomaterials, resulting in cellulose-based porous PCMs with tailored properties, offering versatility and applicability in various fields such as papermaking, textiles, and renewable biofuel production [115].

It is known that gels could possess various unique properties due to their structural advantages [117-119]. Chen *et al*. [120] utilized fresh cuttlefish ink as a primary material for obtaining natural melanin particles. Melanin, known for its effectiveness in combating ultraviolet rays, operates by swiftly vibrating its chemical chain, thereby converting harmful ultraviolet rays into harmless heat. Leveraging this property, cellulose nanofibers (CNF)/melanin hybrid aerogels were fabricated by integrating melanin particles with CNF. Subsequently, PEG was vacuum-immersed into the aerogel to yield the CPCMs. The melting enthalpies of the CPCMs ranged from 168.3 to 175.9 J/g, with the incorporation of melanin exhibiting minimal impact on the energy storage density of the prepared CPCMs. Tests conducted under artificial sunlight revealed a noteworthy improvement in CPCM photothermal conversion efficiency, which increased to 85.9%. Furthermore, thermal cycling tests and thermogravimetric analysis (TGA) attested to the excellent thermal stability and robust encapsulation ability of CPCMs.

The hydrophilic nature of cellulose aerogels hinders their TES potential, as they have weak interaction with n-alkanes, resulting in ineffective impregnation and storage. Additionally, their low thermal conductivity and inefficient heat transfer properties limit their practical applicability. In efforts to enhance both the loading rate of n-alkanes and thermal conductivity within cellulose aerogels, Du and colleagues [121] embarked on the development of FSPCMs. Their process involved impregnating n-octacosane into alkylated nanofibrillated cellulose (NFC)/carbon nanotubes (CNT) (NFC/CNT) hybrid aerogels (ANCAs) as depicted in Figure 4a. The resulting three-dimensional porous aerogels were interconnected and showed promise

in containing melted n-octacosane while reducing the risk of leakage caused by surface tension and a strong wicking effect. The alkylated alteration resulted in a notable increase in the affinity between NFC/CNT aerogels and n-alkanes, which led to enhanced loading capacity, better shape stability, and increased thermal reliability for the CPCMs. Notably, the NFC/CNT aerogels exhibited a notable increase in loading rate, escalating from 26.1% to 38.7% with the augmentation of multi-walled CNTs (MWCNT) weight percentage from 6% to 18%, as illustrated in Figure 4b. Specifically, samples denoted as CPCM-6, CPCM-12, and CPCM-18 corresponded to MWCNT weight percentages of 6%, 12%, and 18%, respectively.

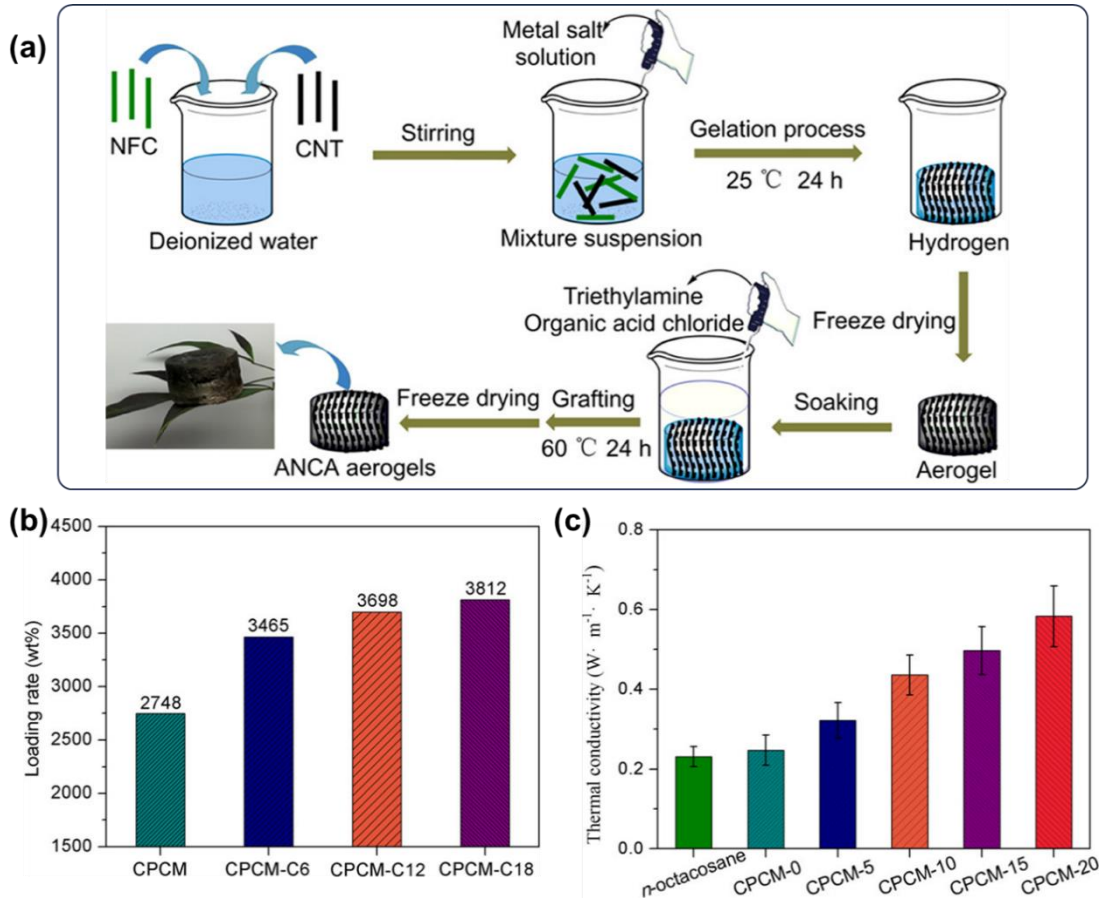


Fig. 4. (a) Schematic illustration of production of alkylated NFC/CNTs hybrid aerogels, (b) Loading capacity n-octacosane for CPCMs, and (c) Thermal conductivity of values of n-octacosane and selected composites. Reproduced with permission from [121] Copyright (2020), American Chemical Society.

The DSC analysis showed that CPCMs based on the alkylated NFC/CNTs aerogels exhibited an extremely high phase change enthalpy ranging from 250.9 to 252.9 J/g. As demonstrated in Figure 4c, the addition of CNTs significantly raised the thermal conductivity from 0.247 to

0.583 W/(m·K) when the weight percentage of MWCNTs was 20%. This increment resulted in an improvement in photothermal conversion and storage efficiency from 46.9 to 83.4%. The wt% of MWCNTs are 0%, 5%. 10%, 15% & and 20% in samples CPCM-0, CPCM-5, CPCM-10, CPCM-15, and CPCM-20, respectively.

Further investigation into NFC-based CPCMs revealed the potential for achieving an impressive 86.7% solar thermal conversion and storage efficiency [122]. Even after subjecting the CPCMs to 100 melting-freezing cycles, the changes in melting (T_m) and freezing (T_f) temperatures did not exceed 0.5 °C, while the alterations in enthalpies of melting (ΔH_m) and freezing (ΔH_f) remained within 2 J/g, underscoring the exceptional stability and durability of the material.

To solve the problems caused by the low impregnation rate of PEG and the restrictions on the thermal conductivity of cellulose aerogels, Du *et al*. [123] pioneered the development of PEG-grafted NFC/graphene hybrid aerogels. This work involved synthesizing PEG-grafted NFC (NFC-*g*-PEG) through a carboxylation-amidation reaction between NFC and methoxypoly (ethylene glycol) amine (MPEG-NH_2). Subsequently, form-stable PEG/NFC-g-PEG/graphene composites (PNPGs) were fabricated by impregnating PEG into NFC-g-PEG/graphene hybrid aerogels (GA/NFC-g-PEG). Samples of hybrid aerogels (PNPGs) were fabricated with varying graphene contents at 0 wt%, 5 wt%, 10 wt%, 15 wt%, and 20 wt%. Correspondingly, the loading rates of PNPGs and PNG-15 were 4363%, 4321%, 4245%, 4198%, 4122%, and 3472%, respectively. An aerogel, denoted as GA-15/NFC, was prepared as a control, containing 15 wt% graphene oxide. From analysis, results revealed that the surface area of PNPGs is 597.8 m^2/g to 621.7 m^2/g, the average pore diameter is 15.7 nm to 16.1 nm, and the pore volume is 0.537 cm^3/g to 0.553 cm^3/g. Notably, the loading rates of PEG for PNPGs were much higher than that of PNG-15, which is the result of the improved affinity of PEG with NFC-g-PEG/graphene aerogel. Moreover, as the weight percentage of graphene in PNPGs increased, there was a corresponding rise in thermal conductivities, escalating from 0.276 W/(m·K) (0 wt%) to 0.761 W/(m·K) (20 wt%).

Melamine foam (MF) is a favored material for crafting 3D interconnected carbon-based structures due to its lightweight nature, high porosity, and exceptional elasticity. Using this material, Wu *et al*. [33] paired it with CNF/graphene nanoplatelet (CG) to create multi-responsive shape-adaptable PCMs. The CG@MF sponges were crafted by dispersing CNF and undergoing repeated dip-coating with CG hybrids. This method endowed the CG@MF/PEG

PCMs with heightened thermal conductivity, as well as the ability to store energy from light/electrical sources and undergo shape variation driven by light/electricity. The CG@MF sponges boasted open macropores, facilitating the impregnation of PEG melts as characterized by SEM. The CG@MF/PEG FSPCMs demonstrated an excellent encapsulation effect, augmented thermal conductivity, and substantial melting enthalpy (178.9 J/g). These FSPCMs also demonstrate an impressive light/electro-driven shape memory effect, which effectively transforms electric or light energy into heat energy and distributes the converted energy in a smooth manner throughout the phase change process.

Another interesting 2D nanomaterial is black phosphorus (BP) nanosheets, representing innovative efficiency in photothermal conversion, expansive surface area, and high thermal conductivity. Du's team [124] crafted a flame-retardant and FSPCM leveraging CNF, BP nanosheets, and n-octacosane. These 2D layered BP nanosheets boast exceptional photothermal properties, achievable through a synthesis process involving ultrasonication-assisted liquid exfoliation of BP crystals, followed by impregnation of n-octacosane into CNF/BP hybrid aerogels to generate CPCMs. The resultant hybrid CNF/BP aerogel boasted a continuous, interconnected honeycomb-like 3D framework, which proved highly conducive for effectively impregnating alkane into the aerogel. The study demonstrated the successful integration of alkane into the CNF/BP aerogel hybrid, demonstrating its exceptional adsorption capacity without any visible boundary. The energy dispersive spectroscopy showed a uniform distribution of C and P elements in the FSPCM, indicating homogeneous BP nanosheet dispersion and porous aerogels supporting n-octacosane, preventing liquid leakage. The FSPCM demonstrated exceptional performance, achieving a 3073% n-octacosane loading rate, increased thermal conductivity, and 87.6% solar-thermal conversion efficiency, with an increasing BP nanosheet content enhancing flame retardancy. Table 2 summarizes key findings to enhance readability and efficiency in the content of this section, which include the carbon source, PCM matrix, form stabilizer, reinforcement strategy, outstanding properties, and purpose.

Table 2. Summary of key findings - carbon source, PCM matrix, form stabilizer, reinforcement strategy, outstanding properties, and purpose.

Carbon source	Form Stabilizer	Reinforcement Preparation	PCM Matrix	Outstanding Properties			Purpose	Key Findings	Ref.
				Melting Temp. (ºC) (Heating/ Cooling)	Latent Heat (J/g) (Heating/ Cooling)	Form-Stability conditions			
Cellulose Derived Carbon Reinforcements									
Cellulose	CNF/polypyrrole hybrid aerogel	• Delignification • Freeze-Drying • Soaking • Stirring • Polymerization • Final freeze-Drying	n-octacosane	65.0-65.6/48.7-51.0	239.4-258.4/235.3-259.3	Minimal changes in melting/freezing points and enthalpies over 100 cycles; Relative Loss < 3.75-8.08%.	Create high-density n-alkanes/cellulose aerogel composites: Exceptional energy storage, photo-thermal conversion	1. CPCMs have high latent heat (239.4–258.4 J/g) and can load n-octacosane up to 96%. 2. CPCMs maintain excellent cyclic and thermal stability even after 50 cycles. 3. Increasing polypyrrole content in PCM composites enhances photothermal conversion efficiency, reaching up to 85.9%.	[80]
Cellulose	CNF/melanin hybrid aerogel	• Centrifugation • Freezing-drying • Stirring • Gelation process • Freeze-drying • Soaking • Vacuum drying	PEG	66.3-69.1/36.0-38.1	167.1-175.9/160.1-164.6	After 100 cycles, CPCMs' melting, and crystallization points only decreased by about 2%.	To improve photothermal conversion efficiency and superior energy storage density	1. Melting enthalpies of CPCMs range from 168.3 to 175.9 J/g. 2. CPCMs achieve up to 85.9% increase in photothermal conversion efficiency in simulated sunlight tests. 3. CPCMs exhibit excellent thermal stability and encapsulation ability, as noted in thermal cycling tests and TGA.	[120]

Cellulose	Alkylated NFC/CNTs hybrid aerogels	• Stirring • Gelation process • Hydrogen • Freeze-drying • Soaking • Grafting • Freeze-drying	n-octacosane	68.2-68.5/48.2-48.7	251.1-252.9/250.9-252.3	Negligible change in points and enthalpies over 100 cycles, Relative Loss < 3.75-8.08%.	Explore CPCMs: Efficient n-alkanes loading, enhanced thermal conductivity	1. CPCMs: Phase change enthalpies 250.9–252.9 J/g. 2. CNT addition: Boosts efficiency, thermal conductivity 0.247 to 0.583 W/(m·K) (152.4% increase)	[121]
Cellulose	NFC aerogel	• Stirring • Cation-induced gelation • Freeze-drying • Vacuum impregnation	n-octacosane	63.8-64.5/56.3-56.9	249.8-263.1/248.3-262.1	PCM stability: Minimal changes after 100 cycles.	Fabricate high enthalpy, shape-stable n-alkane PCMs	1. PCMs: High enthalpy, reliable thermal performance. 2. Solar efficiency up to 86.7%. 3. PCM durability: Minimal changes after 100 cycles.	[122]
Cellulose	PEG-grafted NFC/hybrid aerogels	• Stirring • Gelation process • Freeze-drying • Impregnation • Freeze-drying	PEG	68.8-69.8/35.2-35.9	187.4-195.5/167.3-173.9	PNPGs: T-50 wt% and Tmax higher than PEG 6000	Develop PCMs: High capacity, conductivity, and solar performance for solar energy	1. CPCMs: PEG, NFC, graphene in aerogels. 2. Aerogels support PEG, prevent leakage. 3. PNPGs: High melting enthalpies. (185.5-187.4 J/g) 4. Graphene boosts efficiency, conductivity in PNPGs.	[123]
Cellulose	CG hybrid-coated melamine foam (CG@MF)	• Stirring • Dispersion • Dip-coating • Vacuum infiltration	PEG	61.7-62.4/ 61.7-62.4	176.6-182.4/ 191.7-192.8	CG5@MF sponge: Constant cyclic stress-strain curves over 100 cycles (50% strain).	Explore FSPCMs: Low rigidity, high conductivity, multi-drive capabilities.	1. CG@MF/PEG FSPCMs: Good encapsulation, enhanced conductivity, high enthalpy (178.9 J/g). 2. Remarkable shape memory effect via phase change. 3. Efficient conversion and storage of light/electric energy. 4. Excellent multi-responsive self-adhesion.	[33]
Cellulose	CNF/BP hybrid aerogels	• Sonication • Stirring • Freeze-Drying	n-octacosane	65.6-66.0/52.0-52.1	248.7-251.6/247.0-250.2	After 100 thermal cycles: Points and enthalpies	Develop CPCMs: Efficient photothermal, enhanced flame	1. CNF/BP aerogels support octacosane, prevent leakage. 2. FSPCM: Thermal storage densities 247.0–251.6 J/g.	[124]

		• Soaking • Vacuum drying				stable, octacosane loading reduced < 4%.	retardancy, good shape-stability.	3. BP increases thermal conductivity, solar efficiency. 4. Increasing BP content enhances flame retardancy.	

2.3 Biofibre Carbon Reinforcements

Unlike other energy storage systems, like thermoelectric [125-128], and battery [129], PCM and its composites have been widely used for thermal energy harvesting. Using biofibre carbon reinforcements in organic PCMs for solar TES could help overcome limitations such as leakage and low thermal conductivity [130]. In this regard, Sheng *et al*. [131] employed inexpensive, sustainable biomass cotton by directly carbonizing to produce 3D carbon sponges, which provide a great supporting and thermally conductive framework for organic PCMs while preserving form stability. In their work, the cotton-derived carbon sponges, made from aerogels, had a highly porous structure with an interconnected network. They further produced paraffin wax (PW)@carbon sponge composites by impregnating the sponges with PW under vacuum, as shown in Figure 5a. The resultant composites offer enhanced heat conductivity of about 0.434 W/(m·K) in Figure 5b, leak-proof form stability, strong cyclability performance (~100 cycles), and a high thermal storage energy density of about (>200 J/g). They ascribed the enhanced energy storage capacity to the entrapment of PCM in the porous matrix depicted in Figures 5c1, c2. Because of their high thermal storage energy density, these SSPCMs may find wide use in thermal energy conversion and storage, especially in solar energy applications.

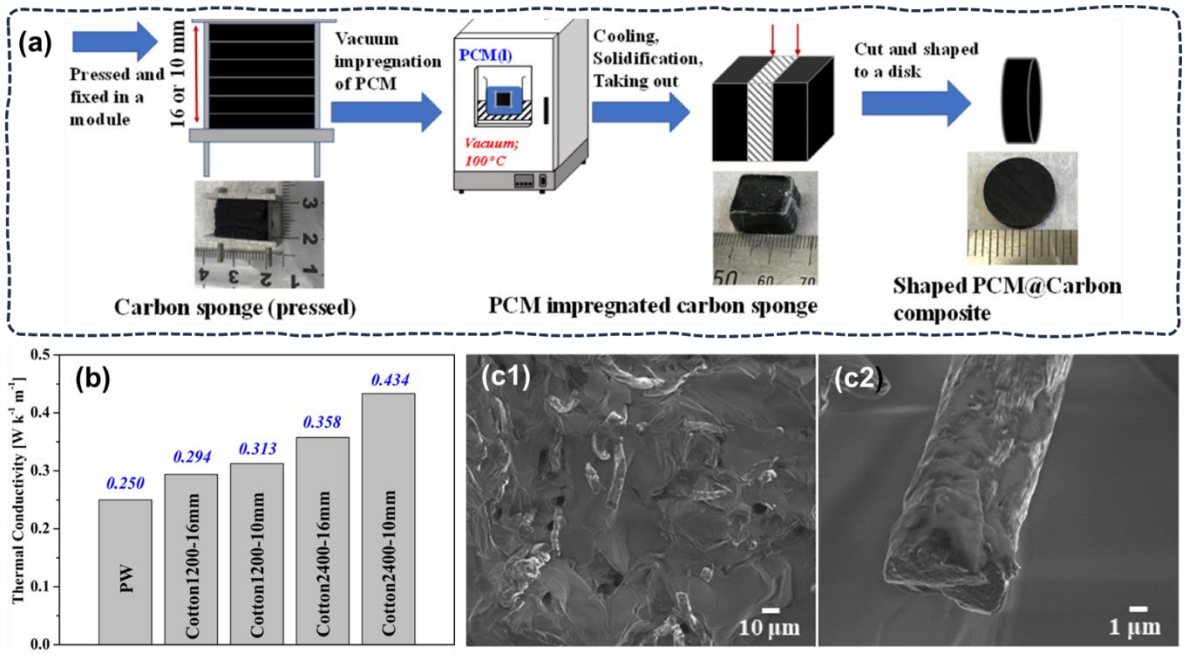


Fig. 5. (a) Illustrative diagram depicting the production process of carbon sponge and PCM/carbon sponge composite, (b) thermal conductivity values of PCM and PW@carbon sponge composites, and (c1, c2) SEM micrographs illustrating typical PCM/carbon composite structures with carbon sponges at 2400 °C. Reproduced with permission from [131] Copyright (2019), Elsevier.

In a similar work [132], the team developed a phase transition material with carbon fibers enclosed by graphene. They rolled a cotton sheet onto a bar, forming a cylinder with aligned fibers, and employed direct pyrolysis and carbonization to create a porous carbon cylinder. Then, CPCMs were fabricated by injecting PW into the carbon scaffolds using vacuum heating. The CPCMs showed excellent shape retention and thermal conductivity with directional preferences. The structural support for the CPCMs is provided by the biomass-derived porous carbon frameworks, which are composed of hollow carbon fibers oriented vertically and graphene. By incorporating 8.5% filler content, the CPCMs demonstrate remarkable thermal conductivity of 1.36 W/(m·K) and 2.68 W/(m·K) along the axial fiber orientation and the lateral fiber direction, respectively. Notably, the increment in the lateral orientation is about 10.7-fold compared with that of pure PW. Furthermore, the CPCMs display robust performance under thermal cycling (~200 cycles), possess high latent heat capacity (199 J/g), maintain structural integrity, and exhibit chemical stability. The results indicate the potential of carbon scaffold-supported CPCMs in thermal energy conversion and management due to their anisotropic thermal conductivity.

Bi's team [133] converted absorbent cotton, a natural biomass, into carbon microtube/graphene hybrid structures by carbonization and continuous chemical vapor deposition of graphene at 1200 °C. The resultant carbon microtube/graphene composite with a hollow tubular configuration was hydrophobic (contact angle ~128°) and with a higher specific surface area (312 m^2/g). This composite was impregnated with organic octadecanoic acid in its structure, resulting in a thermal conductivity of 0.69 W/(m·K) at a 10% carbon microtube/graphene content. The composite also showed a heat storage capacity of 174 J/g, closer to octadecanoic acid alone. More importantly, the composite demonstrated reliable thermal performance even after 500 melting/freezing cycles. This approach offers insights into designing and fabricating carbon microtube/graphene hybrid structures from natural resources.

In another work, Umair's group [134] developed FSPCMs that can be driven by electricity and light. First, the authors treated raw cotton with alkaline and then pyrolyzed at 900 °C to produce a hollow carbon fiber scaffold. Then, they infiltrated PW into a 3D carbon scaffold, effectively trapping up to 85% of PW. The resulting composites demonstrate even heat distribution and maintain their shape during phase change, exhibiting a high energy storage density of up to 182.22 J/g. Additionally, the interconnected hollow carbon fibers possess graphitic properties,

offering both thermal (0.40 W/(m·K)) and electrical conductivity (19.6 S/m) within the PCM matrix. Consequently, the hollow carbon fiber-PW composite shows exceptional energy conversion and storage efficiencies, particularly under low input voltage and light intensity conditions. For instance, the storage efficiency of harvested photo energy stored as thermal energy was 76.4%. These findings represent significant advancements in leveraging biomass-derived materials to enhance photo- and electro-driven PCM technologies for the thermal management of buildings.

Nanomaterials can be used to tune the physical properties of the composites [135-137]. Zhu and colleagues [138] also prepared highly porous 1D-aligned SiC-coated carbon fibers as support scaffolds for paraffin. First, a cylindrical shape of absorbent cotton sheets was formed, sliced into smaller segments, filled with a mixture of silicon sources, and subjected to pyrolysis and calcination under an Ar atmosphere to create SiC-coated carbon scaffolds. Then, the cotton fibers transformed into carbon fibers and reacted with the silicon sources at elevated temperatures, forming a SiC coating on each carbon fiber's surface. The biomass carbon-supported CPCMs exhibit improved heat transmission and anti-leakage characteristics. With a filler ratio of 10.4%, they achieved high thermal conductivity values of 0.61 W/(m·K) in the axial direction and 0.48 W/(m·K) in the lateral direction. The composite also has a substantial heat storage capacity of 186 J/g, making it promising for thermal management applications.

In an interesting study, Sheng *et al*. [139] directly carbonized carbon fibers from biomass (sisal), resulting in porous and honeycomb-like composites. By incorporating PW into the carbon fiber scaffold via vacuum impregnation, FSPCMs were produced. These composites showed about an 8-fold increase in thermal conductivity (1.73 W/(m·K)) compared to pure PW (0.25 W/(m·K)). They also showed notable latent heat capacity (192.2 J/g), good shape retention, thermal stability, and recyclability. The composites also displayed anisotropic thermal conductivity due to the one-dimensional alignment of carbon fiber bundles. These findings suggest the use of cost-effective sisal-derived carbon fibers in TES systems.

2.4 Agricultural residues-Derived Carbon Reinforcements

Agro-residue carbon matrices offer advantages like natural porosity and structural robustness for PCMs, enhancing thermal conductivity and heat transfer [140-142]. This approach promotes sustainability, reduces environmental impact, and aligns with green chemistry and the circular economy, optimizing TES systems and utilizing renewable resources in material

science applications [143-145]. In this context, Gao *et al*. [146] explored using cabbage mustard biochar as a scaffold for tetradecanoic acid in creating SSPCMs. By employing this approach, they significantly increased the thermal conductivity of the SSPCM, reaching 0.597 W/(m·K), which surpassed most biochar-based SSPCMs. The tetradecanoic acid/cabbage mustard biochar SSPCM resulted in a loading capacity of about 57% for tetradecanoic acid and a substantial phase change enthalpy of 103.55 J/g, making it an attractive energy storage material for practical applications. The authors highlighted the accessibility of cabbage mustard biochar from cabbage mustard agricultural waste.

In another work [147], a new type of sustainable carbon material was created using carrots through a hydrothermal reaction and carbonization method. The authors then incorporated PA into the carrot-derived carbon material (CCM) to create PA@CCM composites. When tested for thermal properties and shape integrity, the resultant composites revealed a PA loading ratio of 85.3% and a high latent heat capacity of 166.4 J /g. The PA@CCM composites showed exceptional shape stability and minimal leakage above PA's melting point, resulting in a 145.5% increase in thermal conductivity compared to pristine PA. Similarly, Zou *et al*. [148] developed carbon aerogels derived from pumpkin (PCA) and carrot (CCA) were synthesized through a hydrothermal process and post-sintering. The CCA sintered at 800 °C had a specific surface area of 33.8 m^2/g, surpassing other aerogels sintered at 1000 °C. The porosity of these aerogels allowed for high loading of PA/thiol-ene resin as a PCM to obtain (50PA/thiol-ene@PCA1000) composite. This composite had enhanced thermal conductivity of 0.149 W/(m·K), about 60.5% higher compared to 50PA/thiol-ene. In addition, the resultant composite revealed a latent heat of 88.26 J/g through DSC analysis.

Another significant agricultural byproduct is spent coffee grounds (SCGs), which are plentiful in the coffee industry due to its widespread trade [149]. These SCGs are now being repurposed to fabricate CPCMs [150]. For example, Hu *et al*. [151] used SCGs to create CPCMs using reduced graphene oxide (RGO). The SCGs@RGO framework was shape-stable and demonstrated enhanced thermal stability, energy storage capacity, reusability, and efficient light-to-heat conversion. The authors found that adding RGO stabilized the shape, addressed leakage issues, and strengthened the porous structure, enabling 60.3 wt% PEG absorption. The modified SCGs also displayed superior light absorption across UV-Vis-NIR, enabling rapid solar TES. These PEG/SCGs@RGO CPCMs show excellent chemical and crystalline stability, making them suitable for thermal management applications.

Corn cobs present an ideal alternative as composite materials due to their cost-effectiveness, sustainability, and ability to enhance thermal conductivity. By repurposing agricultural by-products, they reduce environmental impact, making them a valuable and versatile solution for various industries. Zhang and coworkers [152] developed FSPCMs by integrating a mixture of LA-SA into carbonized corn cob (CNCC). Their strategy enhanced the thermal conductivity of the composite, with the composite retaining 77.9% of LA-SA without leakage. Moreover, DSC analysis revealed exceptional thermal properties, with an 87.5% increase in thermal conductivity compared to LA-SA alone. Further DSC analyses confirmed the material's melting point at 35.1 °C with a latent heat of 148.3 J/g and solidification at 29.7 °C with a latent heat of 144.2 J/g. The LA-SA/CNCC FSPCMs carbonized maize straw holds great promise for energy-efficient solutions, especially in building applications. Wen's group [153] utilized carbonized maize straw as a support scaffold for PCM. First, the authors carbonized maize straw biomass and then synthesized the CPCM using a vacuum impregnation of SA. The resultant SA/carbonized maize straw composite showed excellent chemical compatibility and thermal properties. With a maximum SA loading capacity of 77.22%, its melting point was 67.62 °C and a freezing point of 65.2 °C. Additionally, the thermal conductivity of SA/carbonized maize straw increased by 0.14 W/(m·K) compared to 0.16 W/(m·K) of pure SA. The CPCM holds significant promise for solar heat energy storage systems and energy-efficient buildings.

Eggplants can be used as carbon material for phase change applications due to their carbon compounds, which can be transformed into a porous structure ideal for gas and liquid adsorption and storage [154]. This porous carbon material can be impregnated with PCMs to create a composite material for TES, electronics temperature control, and thermal regulation clothing. Zhang *et al*. [155] prepared nano-Ag coated eggplant-based biological porous carbon (BPC) as a support material for loading PEG to overcome challenges like leakage and low thermal conductivity of PCM. They reported that the SSPCM derived from caky BPC showed superior anti-leakage properties and light-to-heat conversion capabilities. The presence of nano-Ag particles significantly increased the support material's thermal conductivity by 40.9%. The composite exhibited exceptional thermal reliability even after 10 thermal cycles. BPC@Ag improved the light-to-heat conversion rate and showed potential for various applications.

In a similar study, Li *et al*. [154] fabricated 3D BPC materials from eggplants as scaffolds for encapsulating PEG in organic PCMs. The BPC, with pores of about 45 μm in diameter, could accommodate high PEG loading and prevent liquid leakage, resulting in a melting enthalpy of

up to 149 J/g. The SSCPCMs showed outstanding thermal cycling properties, retaining 96.3% of their performance after 50 cycles. The BPC's hierarchical porous structure enhanced thermal conductivity by providing an efficient network channel for phonon thermal motion. Moreover, it enhanced the efficiency of CPCMs' solar-to-thermal conversion by functioning as an effective photon catcher and molecular heater. Through an affordable preparation procedure, the BPC provides potential applications in PCMs.

Rice husk ash is a promising porous support material for PCMs such as PW etc., due to its abundant pores and light absorption properties. To address the potential PCM leakage issues, Yu's group [156] explored rice husk ash (RHA) as an FSPCM for encapsulating PW as shown in Figure 6a. They employed a two-step method, which resulted in a nanoporous structure with strong PW adsorption capabilities.

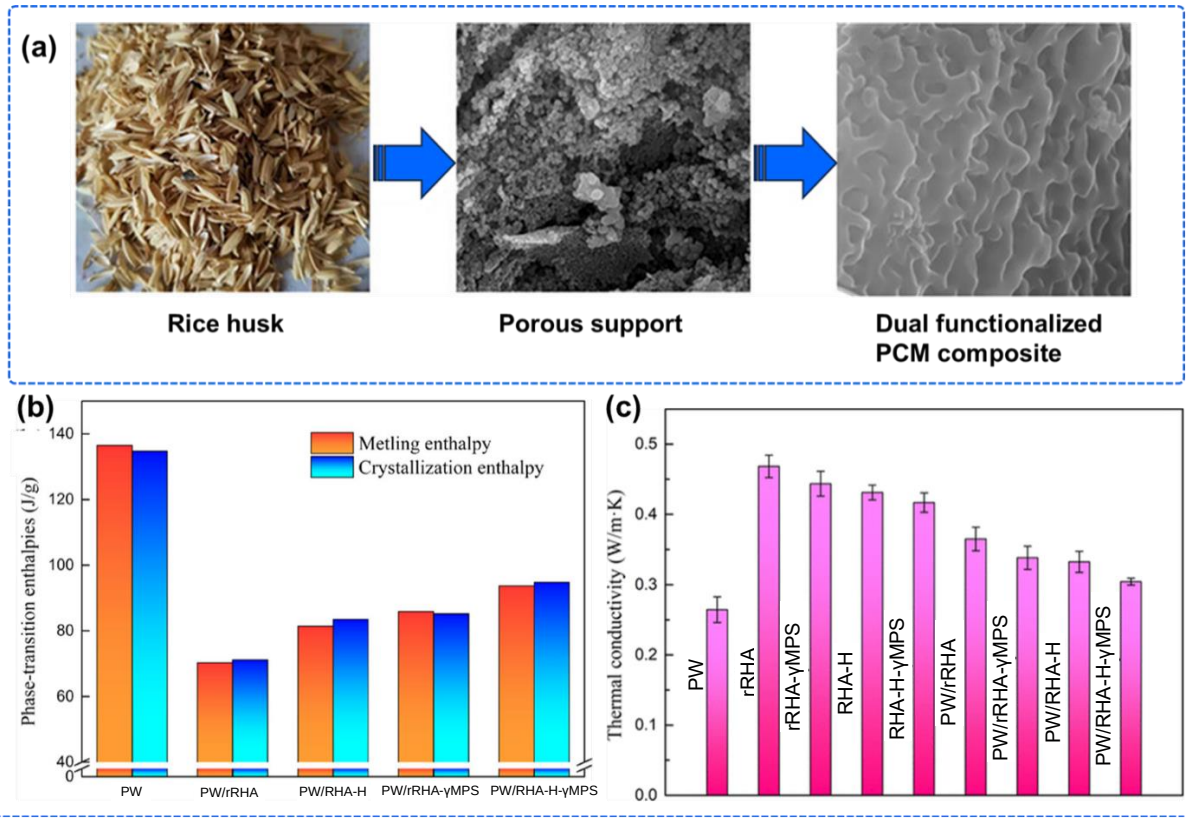


Fig. 6. (a) Schematic illustration of hydrophobic modification process of rough RHA (rRHA) and RHA-H with γ-MPS, (b) phase transition enthalpies of PW, PW/rRHA, PW/RHA-H, PW/rRHA-γMPS, and PW/RHA-H-γMPS and (c) Thermal conductivities of PW, rRHA, rRHA-γMPS, RHA-H, RHA-H-γMPS, PW/rRHA, PW/RHA-H, PW/rRHA-γMPS, and PW/RHA-H-γMPS at 20 °C. Reproduced with permission from [156] Copyright (2021), American Chemical Society.

The first stage involved a neutralization reaction followed by chemical grafting of hydrophobic γ-(methacryloyloxy) propyltrimethoxysilane (γ-MPS, KH-570). The porous PW/RHA-H-γMPS composite demonstrated a higher retention capacity of 70.1%, surpassing untreated RHA and RHA modified with hydrochloric acid or silane coupling agent. Additionally, figure 6b revealed PW/rRHA) had the lowest melting and crystallization enthalpies, while PW/rRHA-γMPS had higher enthalpies, indicating a 14.4% and 14.5% increase in melting and crystallization. The PW/RHA-H-γMPS composite demonstrated a high heat storage capacity of 95.7 J/g and excellent light-to-thermal conversion efficiency. This increase was ascribed to the grafting of γMPS onto amorphous silica within rRHA. As shown in Figure 6c, the thermal conductivities of PW/rRHA, PW/RHA-H, PW/rRHA-γMPS, and PW/RHA-H-γMPS values are 0.3649, 0.3382, 0.3324, and 0.3043 W/(m·K), respectively. All four bio-based RHA form-stable PWs show enhanced thermal conductivity compared to PW due to their superior heat transfer capabilities.

Repurposing biomass waste, such as watermelon rinds, exemplifies resource efficiency and environmental stewardship by reducing chemical inputs and providing an economically viable material for sustainable energy solutions [157]. Liu and colleagues[158] created composites with mannitol and carbonaceous aerogel generated from sustainable biomass for effective thermal energy release and stable form preservation. The resultant composites, derived from watermelon rind waste, have unique attributes like lightweight nature, porosity, and oxygen-rich groups. They processed the watermelon rind waste via a hydrothermal carbonization route to obtain biomass-derived carbonaceous aerogel (BDCA). Then, they introduced the molten mannitol by vacuum impregnation at a temperature of 190 °C for 6 h, followed by gradual cooling to room temperature. The authors reported that the final composites had a high thermal energy capacity of 280 J/g, enhanced thermal conductivity (>1 W/(m·K)), robust thermal stability, shape integrity, and resistance to thermal cycling. When BDCA loading exceeds 9 wt%, the thermal-energy-release efficiency exceeds 95%. Their work presents a promising avenue for fabricating phase-change composites based on sugar alcohols, offering high TES density and efficient energy release for medium-temperature TES applications [158]. A salt-based PCM solar photothermal energy storage solution has been developed by the same group [157] using sodium acetate trihydrate (SAT) as a PCM, carboxymethylcellulose (CMC) and biomass-derived carbonaceous sheets (BDCSs). These sheets, sourced from watermelon rind waste, have a layered structure, smooth surface, and a high concentration of functional -OH

groups. They reported that the SAT-based composite system had a remarkable thermal energy capacity of 212.2 J/g and a solar energy conversion efficiency of 80.18%. Furthermore, it also exhibited excellent thermal conductance, maintains shape stability without phase segregation, and exhibits remarkable thermal cycle stability.

Wang *et al*. [35] developed SSPCMs using biomass carbon aerogels (BCAs) as the host matrix, as shown in Figure 7a, achieving remarkable light-to-thermal efficiency ranging from 67.8% to 75.6%. The receptacle (r-CA) and stem (s-CA) aerogels from sunflower biomass were impregnated with hexadecylamine (HDA) (Figure 7b) and exhibited an unprecedented loading rate of within BCAs, reaching up to 1988% and 873% by weight and volume, respectively.

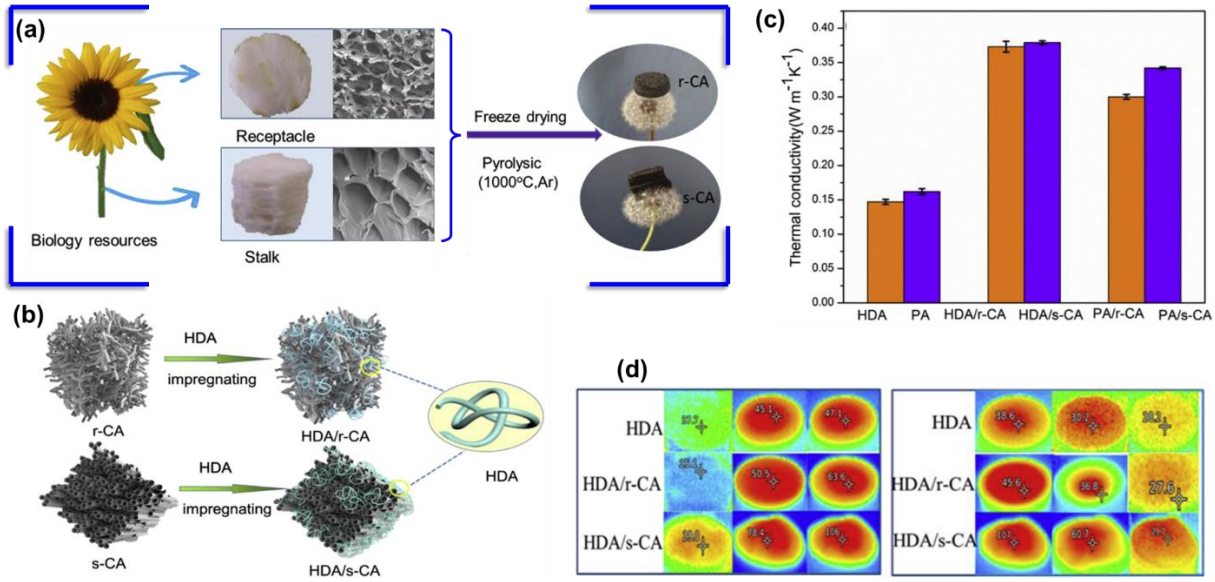


Fig. 7. (a) Schematic illustration of r-CA and s-CA preparation, (b) Impregnation process of HDA/r-CA and HDA/s-CA CPCMs, (c) Thermal conductivity of the HDA and HDA/r-CA and HDA/s-CA CPCMs, and (d) Infrared images of the HDA, HDA/r-CA and the HDA/r-CA under 1 sun irradiation, respectively. Reproduced with permission from [35] Copyright (2020), Elsevier.

They further analyzed the thermal conductivity of pure PCM and synthesized CPCMs. HDA showed a thermal conductivity of 0.147 W/(m·K), while HDA/r-CA and HDA/s-CA showed higher values, 2.54 and 0.379 W/(m·K), respectively, as depicted in Figure 7c. PA/r-CA and PA/s-CA showed higher thermal conductivities, 1.85 times that of pure PA. This improvement is due to the high thermal conductivity of BCAs and their porous carbon network structure, allowing rapid heat transfer without additional nanoparticles. Additionally, infrared images in

Figure 7d show that HDA/r-CA exhibits greater efficiency than HDA/s-CA. This enhancement was attributed to its higher phase change enthalpy, particularly in converting light into thermal energy and storing it under simulated solar conditions (100 mW/cm^2).

Sugar [159] and sugarcane biomass [160] are promising carbon materials in composite fabrication for PCM applications due to their high surface area, thermal conductivity, and stability. Sun *et al.* [159] employed a new method for creating hierarchical porous carbon (HPC) from materials like sucrose and sodium bicarbonate. This HPC (surface area ~1118 m^2/g) acts as a scaffold for PW, creating CPCMs (HPC–PW CPCMs) with exceptional solar-thermal conversion properties. The HPC-PW CPCMs, with a loading capacity of about 83.96%, have exceptional heat transfer, shape retention, cyclic stability, and sunlight absorption capabilities. Moreover, the composites maintained a stable phase-change enthalpy of 152 J/g even after 1000 heating-cooling cycles while achieving an impressive solar-thermal conversion efficiency of up to 89% under 300 mW/cm^2 irradiation.

Likewise, Su and coworkers [161] constructed a functional heat storage unit by preparing carbonized (310/PEG) and non-carbonized (NC/PEG) sugarcane-based SSPCMs using the vacuum impregnation method. The authors found that the distinctive channel structure was essential for heat storage and resulted in thermal stability due to the absence of chemical reactions between PEG and sugarcane-based biomass. The results showed that they exhibited outstanding shape-stabilized phase transition behavior, with an enthalpy efficiency of 94.84%, a high melting enthalpy of around 140.04 J/g, and a better thermal conductivity of nearly 28% above PEG. The directed heat conduction skeletons and open channels were found to be responsible for the higher performance, which suggests that they might be used in energy devices.

3. Artificial biomaterials-stabilized phase change materials

Diatoms, abundant in oceanic and freshwater environments, offer a renewable and abundant carbon source for PCMs [60, 162]. Their large surface area allows efficient heat transfer during phase change, and their chemical stability and biocompatibility make them a suitable choice for PCM applications [163, 164]. Incorporating artificial diatom frustule into PCMs could improve TES systems in building insulation, electronics, and solar energy [165].

Wu *et al*. [63] employed artificially cultured ship-shaped diatoms have been used as a supporting material for SSPCMs as shown in Figure 8a, demonstrating remarkable absorption capabilities and high latent heat. In their work, they first calcined the diatoms to create

sufficient porosity and increase the surface area for PEG impregnation. As seen in Figure 8c, the calcined diatom frustules (CDF) calcined at 400 °C exhibited a high specific surface area of 155.9 m^2/g while retaining a distinct skeletal structure. Moreover, the PEG/400CDF SSPCMs had a high capacity of approximately 72.7%, reaching up to 128.9 J/g and a relative enthalpy efficiency of 97.7%. To understand the thermal-to-thermal energy conversion of the composites, PEG/800CDF exhibited a higher surface temperature increase compared to PEG/400CDF, indicating increased thermal energy retention, thereby enhancing its ability to effectively impede heat spread corresponding to the infrared images in Figure 8b.

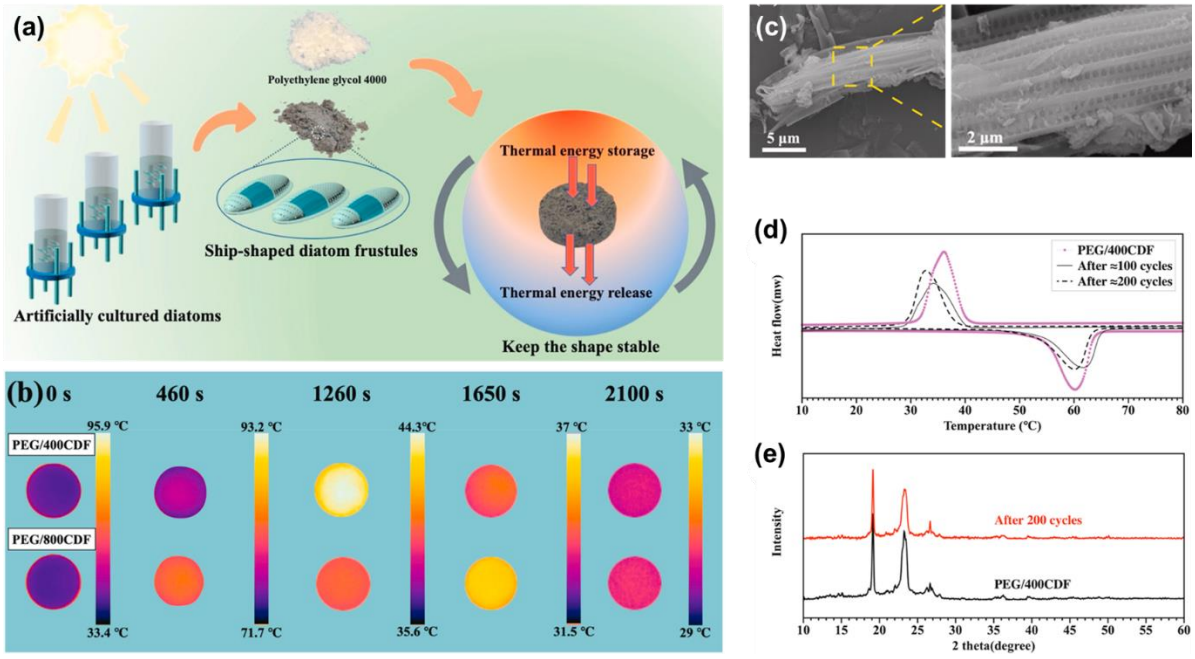


Fig. 8. (a) Schematic diagram detailing the fabrication process of ship-shaped diatom frustules (DFs) SSPCMs. (b) infrared images of the analysis, (c) SEM micrograph of 400CDF, (d) DSC curves, and (e) XRD spectra of PEG/400CDF. Reproduced with permission from [63] Copyright (2021), Elsevier.

Moreover, thermal cycles show no molten PEG seepage in 400CDF/PEG composites (Figure 8d), making them suitable for TES applications. XRD testing showed no discernible difference after 200 cycles, indicating the resilience of PEG's crystal structure within the composite (Figure 8e). This breakthrough demonstrates the potential of unconventional materials in PCM applications and their viability for TES solutions.

Polymers have been widely used in various applications due to their network property [166-169]. In a similar work, Huang's group [62] synthesized diatom materials through artificial cultivation, acid pickling, and sintering processes. Despite the reduction of PEG's crystalline areas, no chemical interaction took place throughout the production process between PEG and the diatom-based biomass. According to analysis techniques, SSPCMs with sintered DF demonstrated good thermal stability and phase change performance in the PEG solid-liquid transition zone,. The melting and crystallization processes yielded maximum latent heat values of roughly 121.54 J/g and 127.20 J/g, respectively. Notably, the relative enthalpy efficiency reached a remarkable ~98.1%. The produced SSPCMs showed dependable heat storage and temperature control, underscoring the promise of artificially cultivated diatom-based biomass in PCMs, especially for temperature control and waste heat recovery.

In another work, Li *et al*. [59] prepared TES coatings using DFs and wax to offer a sustainable solution for energy management. The authors reported that these coatings, coated with silver nanoparticles, had a remarkable thermal conductivity of 0.87 W/(m·K), allowing efficient heat transfer and storage. The micro/nanostructured surface of DFs and the low-surface-energy wax provide superhydrophobicity, enhancing resistance against moisture intrusion. When these coatings with a melting enthalpy of 114.27 J/g were applied using a spray-coating technique, they adsorbed about 55 wt% of PW without leakage. Their high energy storage density, improved thermal conductivity, and scalability make them versatile solutions.

In another study, Sun's team [170] presented a superhydrophobic TES coating, a fully biomass-based SSPCM that uses beeswax (BW) as the PCM and DFs as supporting structures. The DFs had exceptional adsorption capacity and high heat storage capacity, accommodating up to 65 wt% BW without leakage, and possessed a high heat storage capacity of 112.57 J/g. The DF/BW coating exhibited robust thermal stability, enduring 500 heating-freezing cycles with less than a 5% reduction in phase change enthalpy. The coating also displayed superhydrophobic properties due to BW's low surface energy and DFs' micro/nanostructures. Table 3 summarizes artificial biomaterials stabilized PCMs, which include the carbon source, form stabilizer, reinforcement preparation, PCM matrix, outstanding properties, purpose, and key findings.

4. Applications of sustainable carbonized biomass-stabilized PCMs

Biomass-stabilized PCMs are distinguished by their use of renewable, eco-friendly materials, making them well-suited for applications where sustainability is a key concern.[53] On the other hand, sustainable carbonized biomass-stabilized PCMs represent a breakthrough in materials science, providing an eco-friendly solution for thermal management. These innovative materials highlight their potential to enhance energy efficiency and promote environmental sustainability.[54] By integrating renewable biomass-derived materials into PCM technology, this approach presents several potential applications across various industries as shown in Figure 9, due to their ability to store and release thermal energy during phase transitions.

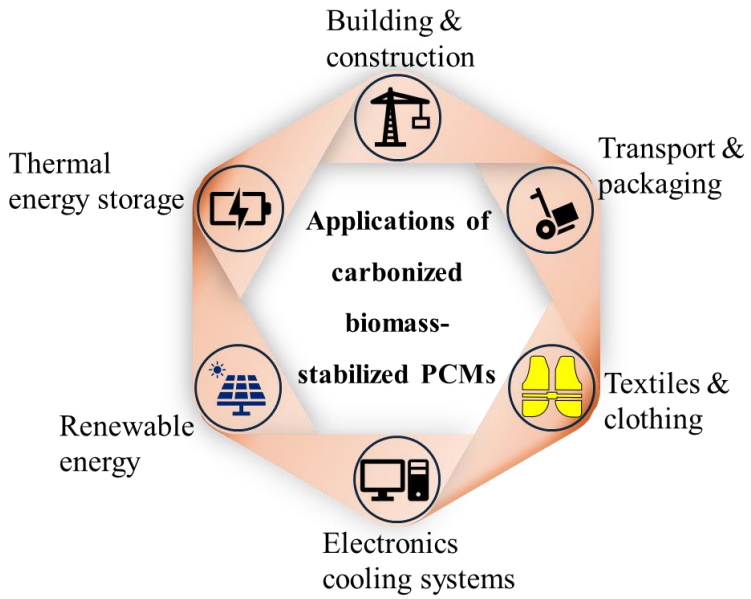


Fig. 9. Applications of sustainable carbonized biomass-stabilized PCMs

These applications include (i) in building and construction, integration of carbonized biomass stabilized PCMs could enhance thermal energy storage and improve energy efficiency in residential and commercial buildings. This includes applications in walls, ceilings, and flooring systems[171]; (ii) in thermal energy storage systems, such as thermal batteries and solar thermal storage, where they can store and release heat efficiently[172]; (iii) In the renewable energy sector, such as solar energy systems, they can store excess heat and improve overall energy management[10]; (iv) electronics cooling systems for electronic devices and components to manage heat dissipation and improve the reliability and performance of electronics[25]; (v) incorporation into textiles and clothing to provide temperature regulation

and improve comfort in smart clothing and outdoor gear[52]; and (vi) use in temperature-sensitive transport and packaging systems, such as in-vehicle batteries and passenger compartments, to manage temperature fluctuations and enhance energy efficiency.[173] By harnessing the benefits of carbonized biomass, these advanced PCMs not only support sustainable development goals but also drive innovation in materials science and energy management.

Table 3. Summary of artificial biomaterials stabilized PCMs including carbon source, PCM matrix, form stabilizer, reinforcement strategy, outstanding properties, and purpose.

Carbon source	Form Stabilizer	Reinforcement Preparation	PCM	Outstanding properties			Purpose	Key Findings	Ref.
				Melting Temp. (ºC) (Heating/ Cooling)	Latent Heat (J/g) (Heating/ Cooling)	Form-Stability conditions			
Agricultural residues-Derived Carbon Reinforcements									
Carrot	CCM	• Peel carrot flesh via hydrothermal reaction. • Freeze-drying • Carbonization at < 750 °C • Pyrolysis @1200 °C	PA	68.4/55.5	166.4/163.1	After 100 cycles, PA@CCM1200 composite loading ratio is 85.3 % and latent heat of 166.4 J/g	To explore the use of carrots as an eco-friendly and economical source for synthesizing CCM for PA impregnation	1. CCM with unique hybrid microstructure. 2. High latent heat capacity of PA@CCM (166.4 J/g) 3. Increased loading ratio of PA@CCM (85.3%) without any visible leakage. 4. Enhanced thermal conductivity (0.54 W/(m·K))	[147]
Carrot and pumpkin	CCA, PCA & thiol-ene resin	• Cutting of the pumpkin (or carrot) flesh • Sanitization of pumpkin (carrot) in hot water & ethanol • Lyophilisation • Sintering	PA	61.2/60.9	94.94/88.86	-	To fabricate a biomass-derived scaffold for PCMs	1. Porous carbon aerogels boost PCM stability. 2. 50PA/thiol-ene@PCA1000 has 60.5% higher conductivity due to carbon aerogels	[148]

SCGs	SCG/graphene oxide powder	• Graphene oxide reduction with L-ascorbic acid • Encapsulate SCG • Dry under vacuum at 80 °C	PEG (M_n = 4000)	62.0/36.0	98.7/95.0	After 100 phase change composite PCMs cycles, PEG/SCGs@RG Organic CPCMs are reusable, chemically, and crystalline stable	To efficiently utilize SCGs in CPCMs	1. SCGs, with 1–5 wt% RGO, stabilize CPCMs, addressing leakage and low light-to-heat conversion. 2. SCGs@RGO improve porous structure, absorb 60.3 wt% PEG, boost leakage resistance, and enhance thermal conductivity. 3. SCGs@RGO absorb UV–Vis–NIR, convert light to heat rapidly, storing solar energy within 245 s.	[151]
Corn cobs	CNCC	• Corn cobs washing • Freeze drying. • Carbonization of corn cobs at 650 °C/3 h.	LA-SA	35.1/29.7	148.3/144.2	LA-SA/CNCC FSPCMs exhibit chemical and structural stability over 200 thermal cycles.	To synthesize FSPCMs by blending LA-SA eutectic with CNCC	1. LA-SA/CNCC FSPCMs prepared for building energy storage. 2. CNCC retains 77.9 wt% LA-SA without leakage. 3. Thermal conductivity of LA-SA/CNCC FSPCMs (0.441 W/(m·K)): 1.93 times higher than LA-SA.	[152]
Eggplant	Nano-Ag coated eggplant-based BPC	• Carbonization at 800 °C/2 h • Electroless plating at 60 °C/16 h • Dry at 60 °C	PEG (M_n = 6000)	59.8/40.3	147.8/143.7	After 10 thermal cycles, SSPCM i.e., BPC@Ag/PEG (95%) showed sustained	To develop nano-Ag coated eggplant BPC to boost thermal conductivity and seal PEG in PCM	1. BPC@Ag/PEG boosts thermal conductivity by 40.9%. 2. BPC@Ag has higher surface area and pore volume.	[155]

						thermal reliability		3. BPC@Ag/PEG shows superior heat storage capacity.	
Eggplant	3D spongy-like BPC	• Hydrothermal carbonization • post-pyrolysis at (800 °C, 900 °C, 1000 °C)	PEG (M_n = 2000)	54.71- 61.55/ 22.76-19.90	121.73-149/ 114.00-138.14	SSPCMs showed outstanding thermal cycling properties, retaining 96.3% after 50 cycles	To fabricate eggplant-derived BPC for PEG encapsulation in SSPCMs	1. BPC with nanopores and macropores allowed high PEG loading (~90.1 wt%). 2. Hierarchical pores prevented liquid leakage, achieving a melting enthalpy of 149 J/g.	[154]
Maize straw	Carbonized maize straw	• Carbonization of maize straw with carbon coke	SA	67.62/ 65.28	160.74/160.47	The SA/carbonized maize straw FSPCM exhibited stability before and after 200 thermal cycles	To utilize carbonized maize straw as a matrix to address PCM leakage and improve thermal conductivity	1. SA loading in SA/carbonized maize straw reached 77.22%, with proper melting/freezing temperatures and high latent heat. 2. SA/ carbonized maize straw exhibits significantly higher thermal conductivity than pure SA. 3. SA/carbonized maize straw reduces melting time by 50% and freezing time by 73% compared to SA.	[153]
RHA	Acid-activated, hydrophobized rRHA-γMPS & RHA-H-γMPS	• rRHA ultrasonic acid-treated activation • Hydrophobic modification of rRHA and	PW	52.1/48.2	80.4/81.5	PW/RHA-H-γMPS maintains phase change properties, is reliable after 300 cycles.	To explore the application of RHA in FSPCMs	1. RHA-H-γMPS holds more PW due to enlarged pore structure and hydrophobic surface. 2. PW/RHA-H-γMPS composite shows	[156]

		RHA-H with γ-MPS						higher heat storage capacity (95.7 J/g)	
Sucrose and sodium bicarbonate	HPC	• Ball-milling • Carbonization 800 °C/3 h	PW	28.00-29.93/ 52.98-53.05	111.78-152.21/ 109.82-148.68	CPCM maintains stable phase transition enthalpy after 1000 cycles	To create porous carbon-based CPCMs for energy storage and solar harvesting using sucrose and sodium bicarbonate	1. Hierarchical porous structure facilitates high surface area and PW loading in shape stabilized CPCM. 2. Maximum loading at 83.96% based on TG measurements. 3. Thermal conductivity boosted by 180% with carbon matrix.	[159]
Sugarcane biomass	Carbonized sugarcane biomass	• Carbonization (600 °C, 800 °C, 1000 °C)	PEG (M_n = 4000)	56.97/35.97 (NC/PEG) & 61.06/35.59 (310/PEG)	130.87/129.45 (NC/PEG) & 140.04/137.54 (310/PEG)	NC/PEG and 310/PEG samples remained stable, no leaks during heating	To develop heat storage with sugarcane materials to improve thermal conductivity and prevent leakage in PCMs	1. Thermal properties measured by DSC: high melting enthalpy (140.04 J/g), 94.84% relative enthalpy efficiency. 2. SSPCMs exhibit 0.297 W/(m·K) thermal conductivity, 28.02% higher than pristine PEG.	[161]
Sunflower	BCAs	• Freeze-drying • Pyrolyzed at 1000 °C/3 h	PA	43.25±1.74-49.81 ±4.05/ 29.52± 6.7-36.12 ± 4.39	270.2 ± 1.07/ 266.9 ± 6.87	PCM/BCAs composites: stable, recyclable; enthalpy unchanged after 50 cycles	To fabricate SSPCMs by impregnation of PCM into biomass carbon aerogels of sunflower	1. HDA/BCAs exhibit high light-thermal conversion efficiency (67.8%-75.6%). 2. Loading rate of HDA in BCAs: up to 1988 wt% and 873%.	[35]
Watermelon rinds	BDCA	• Hydrothermal method • Carbonation	Mannitol	-	281.9-255.5/ 258.3-249.5	Loaded mannitol retains its chemical structure after 200 thermal cycles	To create BDCA/mannitol phase-change composites via vacuum impregnation	1. BDCA/mannitol composites: High latent heat, less supercooling, improved thermal conductance.	[158]

								2. 9 and 12 wt% BDCA yields >95% thermal-energy-release efficiency	
Watermelon rinds	BDCSs & CMC	• Hydrothermal method • Carbonation • Freeze drying.	SAT	63.00/60.5	240-210/ supercooling of 0.9 °C	SAT/CMC/BDCSs composite showed only a 5.0% decrease in melting enthalpy after 500 thermal cycles	To develop efficient phase-change system with SAT and BDCSs for solar energy storage	1. Solar photothermal conversion efficiency of SAT/CMC/BDCSs composite: 80.18%, 53.7% higher than pure SAT. 2. SAT/CMC/BDCSs composite: High thermal energy capacity of 212.2 J/g.	[157]
Artificial Biomaterials for PCM Reinforcement									
Artificially cultured ship-shaped diatoms	CDF	• Acid pickling • Centrifuge • Calcination @ 400 °C, 800 °C for 2 h	PEG4000	54.3/40.0	128.9/136.7	After 200 cycles, crystallization enthalpy: 131.2 J/g, fusion enthalpy: 124.0 J/g, <4% latent heat change	To use ship-shaped diatoms to improve the thermal properties of PEG/CDF SSPCMs for geothermal panels & insulation	1. Cultured ship-shaped diatoms used for SSPCMs. 2. SSPCMs absorb high capacity. 3. SSPCMs have a latent heat of 128.9 J/g. 4. SSPCMs achieve 97.7% enthalpy efficiency.	[63]
Artificially cultured diatoms	Sintered DFs	• Acid pickling • Sintering @600 °C/2 h	PEG4000	57.87/27.51	112.89/118.51	After 200 thermal cycles, PEG/sintered DFs show minor changes in melting enthalpy (ΔHm) (7.12%) and crystallization enthalpy (ΔHc) (6.83%)	To utilize cultured diatoms as support for high-performance SSPCMs, using different DFs forms and PEG, with emphasis on stability and energy storage. behavior	1. PCMs from cultured diatoms for the first time. 2. Composite shows excellent performance. 3. Relative enthalpy efficiency reaches ~98.1%.	[62]

Artificially cultured diatoms	CDFs	• Calcination	BW	59.03-59.82/52.79-51.33	91.00-120.77/82.07-110.49	The thermal stability test reveals that the DF/BW coating can endure 500 heating-freezing cycles with a phase change enthalpy reduction of less than 5%	To develop superhydrophobic thermal coatings with self-healing, using PCMs and a protective agent, for various applications	1. DFs combine securely with BW, achieving a 65 wt% adsorption capacity without leakage. 2. TGA testing indicates that DFs elevate BW's onset decomposition temperature to ~250 °C in all DF/BW coatings. 3. Superhydrophobic TES coatings recover swiftly with heating at 80 °C for 20 min, enduring 20 damage-repair cycles post harsh conditions exposure.	[170]

5. Challenges, Existing research gaps and Future directions

5.1 Challenges in the real applications of PCM-integrated building designs/systems

Phase change materials (PCMs), including biochar-stabilized ones, offer potential benefits for building designs due to their sustainability and beneficial thermal properties.[174, 175] Despite these advantages, real applications of integrating PCMs into building systems presents several challenges. Some key issues include biochar's low thermal conductivity, affecting heat transfer efficiency and overall performance.[176, 177] Moreover, integrating biochar with existing building materials can be complex, requiring careful consideration to ensure compatibility and maintain structural integrity. Additionally, the long-term stability and durability of PCMs can be a concern, with factors such as degradation and moisture interaction potentially compromising performance.[178] Addressing the challenges of integrating phase change materials (PCMs) into building designs requires innovative approaches.[179] Flammability is another major concern for building materials, which has prompted advancements in developing fire retardants for biochar-based PCMs.[180, 181]

5.2 Fire prevention technology in reinforced composite PCMs

To mitigate the flammability risks associated with PCMs, researchers have focused on reinforcing these materials with fire-resistant technologies.[178] Specifically, research includes (i) incorporation of fire-retardant additives (halogenated compounds, phosphorus-based agents, inorganic fillers) to enhance the fire resistance of PCMs[182], (ii) modification of matrices with fire-resistant polymers or blends, (iii) use of barrier technologies such as intumescent coatings, and use of nanomaterials (nanoclays and carbon nanotubes) to enhance the fire resistance of PCMs.[183] For instance, Zou *et al.*[184] prepared flame retardant PCM by mixing pentaerythritol phosphate (PEPA) and phosphorus-grafted hexadecanol. In their work, they reported that the phosphorous-treated blended PCM quickly releases phosphorus-free radicals and phosphoric acid during burning, reducing peak heat release rate (PHRR) and total heat release (THR). Moreover, the fire performance index (FPI) for the sample was high at about 0.209 m^2s/kW, attributed to the synergistic effect of PEPA and the phosphorus groups. This higher FPI value suggests a longer time before the release of flammable gases, thereby providing more time for escape in case of a fire. These innovations have not only enhanced safety but also led to significant improvements in thermal energy storage, optimizing the effectiveness of PCMs in building systems.[171]

5.3 Existing research gaps and Future directions

Advancing the use of biomass carbonized materials in PCMs comes with several challenges. One major issue is that the thermal performance of these PCMs can differ depending on the type of biomass and how it's processed.[102] This means researchers must ensure consistency in performance by standardizing the carbonization process and thoroughly understanding how different biomass sources affect thermal properties.[153] Additionally, ensuring the long-term stability and durability of biomass-stabilized PCMs is critical, especially for applications exposed to varying environmental conditions. Therefore, long-term stability and durability must be addressed through accelerated aging tests and advanced encapsulation techniques. Next, scaling up the production of biomass-stabilized PCMs while keeping costs competitive with synthetic alternatives can be challenging.[103] To expand production while maintaining cost-effectiveness, researchers need to develop scalable manufacturing processes and economic feasibility studies. Moreover, comprehensive life-cycle analysis is essential to evaluate environmental impacts and end-of-life solutions.[185] More importantly, tailoring PCMs for specific applications demands targeted research and customization, while market adoption can be accelerated through demonstration projects and industry collaboration.[46] Addressing these areas will help advance sustainable and efficient PCM solutions.

6. Conclusion

PCMs hold promise for addressing this challenge, offering high energy density and thermal storage capabilities. However, challenges such as leakage and limited thermal conductivity necessitate developing innovative solutions. FSPCMs, reinforced with natural-derived and carbonized materials, represent a significant advancement in PCM technology, offering enhanced performance and sustainability. Additionally, innovative approaches such as integrating artificially cultured diatoms present exciting opportunities for further innovation in energy storage materials.

In this review, using carbonized biomass materials, including wood, cellulose, agro-waste residues, biofibers, and artificially cultured diatoms, in PCM development has shown their numerous benefits to composites over their uncarbonized counterparts. Noteworthy, carbonization enhances stability and durability by eliminating volatile components, making them more resilient to degradation. It also increases mechanical strength due to the removal of weaker components and the formation of carbon bonds. This makes carbonized materials ideal

for applications in energy storage devices. Carbonization also allows for precise control over porosity and surface area, making them suitable for various processes like adsorption, encapsulation, and impregnation of PCM. With advanced manufacturing techniques like pyrolysis and hydrothermal carbonization methods, further optimization of carbonized biomass materials and artificial diatoms has become possible.

By leveraging these advancements, researchers aim to move the needle in adopting PCM-based energy storage systems, contributing to a more sustainable and resilient energy future. Future research will focus on functionalizing and modifying carbonized material surfaces to confer specific functionalities, expanding their application domains. Carbonized biomass material application in PCM holds promise in sustainable energy solutions and environmental remediation.

Abbreviations

BCAs	Biomass carbon aerogels
BDCA	Biomass-derived carbonaceous aerogel
BDCSs	Biomass-derived carbonaceous sheets
BN	Boron nitride
BP	Black phosphorus
BPC	Biological porous carbon
BW	Beeswax
CA	Capric acid
CCM	Carrot-derived carbon material
CDs	Carbon dots
CDF	Calcined diatom frustules
CMC	Carboxymethylcellulose
CNCC	Carbonized corn cob
CNF	Cellulose nanofibers
CNTs	Carbon nanotubes
CPCMs	Composite phase change materials
CW	Carbonized wood
DFs	Diatom frustules

DPW	Paulownia chips
DSC	Differential scanning calorimetry
DW	Delignified wood
FSPCMs	Form-stable phase change materials
FTIR	Fourier transform infrared spectroscopy
HDA	Hexadecylamine
HPC	Hierarchical porous carbon
LA	Lauric acid
MA	Myristic acid
MF	Melamine foam
MWCNTs	multi-walled carbon nanotubes
NFC	Nanofibrillated cellulose
O-Dt	Organic diatomite
PA	Palmitic acid
PB	Pinecone biochar
PCMs	Phase change materials
PEG	Polyethylene glycol
PW	Paraffin wax
rRHA	Rough RHA
RGO	Reduced graphene oxide
RHA	Rice husk ash
SA	Stearic acid
SAT	Sodium acetate trihydrate
SCGs	Spent coffee grounds
SEM	Scanning electron microscopy
SSPCM	Shape-stabilized phase change material
TES	Thermal energy storage
TGA	Thermogravimetric analysis
WF	Wood flour
WPC	Wood-plastic composites
XRD	X-ray diffraction

Declaration of interests

The authors declare that they have no known competing financial interests or personal relationships that could have appeared to influence the work reported in this paper.

Data availability

No data was used for the research described in the article.

Acknowledgments

This research is supported by the National Research Foundation (NRF) Singapore under its Low-Carbon Energy Research (Grant Reference No.: U2305D4001).

References

[1] D. Keiner, A. Gulagi, C. Breyer, Energy demand estimation using a pre-processing macro-economic modelling tool for 21st century transition analyses, Energy 272 (2023) 127199.
[2] S. Jiao, M. Liu, Y. Li, H. Abrha, J. Wang, Y. Dai, J. Li, N. Kang, Y. Li, X. Liu, Emerging hydrovoltaic technology based on carbon black and porous carbon materials: A mini review, Carbon 193 (2022) 339-355.
[3] A.I. Osman, L. Chen, M. Yang, G. Msigwa, M. Farghali, S. Fawzy, D.W. Rooney, P.-S. Yap, Cost, environmental impact, and resilience of renewable energy under a changing climate: a review, Environmental Chemistry Letters 21(2) (2023) 741-764.
[4] Q. Hassan, P. Viktor, T.J. Al-Musawi, B.M. Ali, S. Algburi, H.M. Alzoubi, A.K. Al-Jiboory, A.Z. Sameen, H.M. Salman, M. Jaszczur, The renewable energy role in the global energy Transformations, Renewable Energy Focus 48 (2024) 100545.
[5] M.M. Rana, M. Uddin, M.R. Sarkar, S.T. Meraj, G. Shafiullah, S. Muyeen, M.A. Islam, T. Jamal, Applications of energy storage systems in power grids with and without renewable energy integration—A comprehensive review, Journal of energy storage 68 (2023) 107811.
[6] S. Khodabakhshi, P.F. Fulvio, E. Andreoli, Carbon black reborn: Structure and chemistry for renewable energy harnessing, Carbon 162 (2020) 604-649.
[7] Z. Zhang, T. Ding, Q. Zhou, Y. Sun, M. Qu, Z. Zeng, Y. Ju, L. Li, K. Wang, F. Chi, A review of technologies and applications on versatile energy storage systems, Renewable and Sustainable Energy Reviews 148 (2021) 111263.
[8] R. Yuksel, N. Karakehya, High energy density biomass-derived activated carbon materials for sustainable energy storage, Carbon 221 (2024) 118934.
[9] P. Wei, M. Abid, H. Adun, D. Kemena Awoh, D. Cai, J.H. Zaini, O. Bamisile, Progress in Energy Storage Technologies and Methods for Renewable Energy Systems Application, Applied Sciences 13(9) (2023) 5626.
[10] A. Panda, A.K. Dauda, H. Chua, R.R. Tan, K.B. Aviso, Recent advances in the integration of renewable energy sources and storage facilities with hybrid power systems, Cleaner Engineering and Technology 12 (2023) 100598.

[11] J. Wu, W.-Y. Wu, S. Wang, D. Kai, E. Ye, W. Thitsartarn, J. Beng, H. Tan, J. Xu, Q. Yan, Polymer electrolytes for flexible zinc-air batteries: Recent progress and future directions, Nano Research (2024) 1-22.
[12] J. Liu, Z. Li, C. Lv, X.-Y. Tan, C. Lee, X.J. Loh, M.H. Chua, Z. Li, H. Pan, J. Chen, Electrocatalytic upgrading of nitrogenous wastes into value-added chemicals: A review, Materials Today (2024).
[13] E. Hu, B.E. Jia, Q. Zhu, J. Xu, X.J. Loh, J. Chen, H. Pan, Q. Yan, Engineering High Voltage Aqueous Aluminum‐Ion Batteries, Small (2024) 2309252.
[14] B.-E. Jia, E. Hu, Z. Hu, J.J. Liew, Z. Hong, Y. Guo, M. Srinivasan, Q. Zhu, J. Xu, J. Chen, Laminated tin–aluminum anodes to build practical aqueous aluminum batteries, Energy Storage Materials 65 (2024) 103141.
[15] J. Mitali, S. Dhinakaran, A. Mohamad, Energy storage systems: A review, Energy Storage and Saving 1(3) (2022) 166-216.
[16] D.S. Jayathunga, H.P. Karunathilake, M. Narayana, S. Witharana, Phase change material (PCM) candidates for latent heat thermal energy storage (LHTES) in concentrated solar power (CSP) based thermal applications - A review, Renewable and Sustainable Energy Reviews 189 (2024) 113904.
[17] P.J. Ong, H.Y.S. Lee, J.C.C. Yeo, Z. Li, J.J.C. Lee, S. Wang, X. Yin, P. Wang, J. Xu, X.J. Loh, A Copolymer of Monomethoxy Poly (ethylene glycol)‐Polycaprolactone as Form‐Stable Phase Change Materials for Thermal Energy Storage, ChemistrySelect 8(39) (2023) e202302997.
[18] F. Odoi-Yorke, R. Opoku, F. Davis, G.Y. Obeng, Optimisation of thermal energy storage systems incorporated with phase change materials for sustainable energy supply: A systematic review, Energy Reports 10 (2023) 2496-2512.
[19] C. Yu, Y.S. Song, Form stable phase change material supported by sensible and thermal controllable thermistor, Composites Communications 40 (2023) 101600.
[20] M.Q. Wu, S. Wu, Y.F. Cai, R.Z. Wang, T.X. Li, Form-stable phase change composites: Preparation, performance, and applications for thermal energy conversion, storage and management, Energy Storage Materials 42 (2021) 380-417.
[21] I.Y. Miranda-Valdez, M.R. Yazdani, T. Mäkinen, S. Coffeng, L. Viitanen, J. Koivisto, M.J. Alava, Cellulose foams as scalable templates for phase change materials, Journal of Energy Storage 73 (2023) 109036.
[22] S. Wang, Q. Huang, Z. Sun, Y. Wang, T. Liang, B. Wang, C. Fan, C. Liu, Porous carbon network-based composite phase change materials with heat storage capacity and thermal management functions, Carbon 226 (2024) 119174.
[23] J.J.C. Lee, S. Sugiarto, P.J. Ong, X.Y.D. Soo, X. Ni, P. Luo, Y.Y.K. Hnin, J.S.Y. See, F. Wei, R. Zheng, Lignin-g-polycaprolactone as a form-stable phase change material for thermal energy storage application, Journal of Energy Storage 56 (2022) 106118.
[24] M.S. Mohtasim, B.K. Das, Biomimetic and bio-derived composite Phase Change Materials for Thermal Energy Storage applications: A thorough analysis and future research directions, Journal of Energy Storage 84 (2024) 110945.
[25] B. Liu, G. Lv, T. Liu, M. Liu, J. Bian, Q. Sun, L. Liao, Research progress of biomass materials in the application of organic phase change energy storage materials, Journal of Materials Chemistry A 12(15) (2024) 8663-8682.
[26] A. Balaji, R. Saravanan, R. Purushothaman, S. Vijayaraj, P. Balasubramanian, Investigation of Thermal Energy Storage (TES) with lotus stem biocomposite block using PCM, Cleaner Engineering and Technology 4 (2021) 100146.
[27] N. Bhardwaj, M. Malik, S. Sundaramurthy, Development of nano-enhanced phase change material from different biomasses for energy application, Journal of Energy Storage 73 (2023) 108837.

[28] Z. Guo, J. Qiu, L. Pel, Y. Zhao, Q. Zhu, J.W. Kwek, L. Zhang, H. Jiang, J. Yang, Z. Qu, A contribution to understanding the rheological measurement, yielding mechanism and structural evolution of fresh cemented paste backfill, Cement and Concrete Composites 143 (2023) 105221.
[29] T.-Y. Lan, H.-I. Mao, C.-W. Chen, Y.-T. Lee, Z.-Y. Yang, J.-L. Luo, P.-R. Li, S.-P. Rwei, A rapid thermal absorption rate and high latent heat enthalpy phase change fiber derived from bio-based low melting point copolyesters, Polymers 14(16) (2022) 3298.
[30] Y. Feng, J. Jiang, Y. Xu, S. Wang, W. An, Q. Chai, U.H. Prova, C. Wang, G. Huang, Biomass derived diverse carbon nanostructure for electrocatalysis, energy conversion and storage, Carbon 211 (2023) 118105.
[31] P. Singh, R. Sharma, M. Khalid, R. Goyal, A. Sarı, V. Tyagi, Evaluation of carbon based-supporting materials for developing form-stable organic phase change materials for thermal energy storage: A review, Solar Energy Materials and Solar Cells 246 (2022) 111896.
[32] H. Sarrafha, A. Kasaeian, M.H. Jahangir, R.A. Taylor, Transient thermal response of multi-walled carbon nanotube phase change materials in building walls, Energy 224 (2021) 120120.
[33] H. Wu, S. Deng, Y. Shao, J. Yang, X. Qi, Y. Wang, Multiresponsive Shape-Adaptable Phase Change Materials with Cellulose Nanofiber/Graphene Nanoplatelet Hybrid-Coated Melamine Foam for Light/Electro-to-Thermal Energy Storage and Utilization, ACS Applied Materials & Interfaces 11(50) (2019) 46851-46863.
[34] X. Chen, P. Cheng, Z. Tang, X. Xu, H. Gao, G. Wang, Carbon-Based Composite Phase Change Materials for Thermal Energy Storage, Transfer, and Conversion, Advanced Science 8(9) (2021) 2001274.
[35] C. Wang, W. Liang, Y. Yang, F. Liu, H. Sun, Z. Zhu, A. Li, Biomass carbon aerogels based shape-stable phase change composites with high light-to-thermal efficiency for energy storage, Renewable Energy 153 (2020) 182-192.
[36] R. Shen, M. Weng, L. Zhang, J. Huang, X. Sheng, Biomass-based carbon aerogel/Fe3O4@PEG phase change composites with satisfactory electromagnetic interference shielding and multi-source driven thermal management in thermal energy storage, Composites Part A: Applied Science and Manufacturing 163 (2022) 107248.
[37] A.G. Olabi, T. Wilberforce, K. Elsaid, E.T. Sayed, M. Ramadan, S.M. Atiqure Rahman, M.A. Abdelkareem, Recent progress on Carbon-based nanomaterial for phase change materials: Prospects and challenges, Thermal Science and Engineering Progress 23 (2021) 100920.
[38] C. Amaral, R. Vicente, P.A.A.P. Marques, A. Barros-Timmons, Phase change materials and carbon nanostructures for thermal energy storage: A literature review, Renewable and Sustainable Energy Reviews 79 (2017) 1212-1228.
[39] Z.-R. Li, N. Hu, L.-W. Fan, Nanocomposite phase change materials for high-performance thermal energy storage: A critical review, Energy Storage Materials 55 (2023) 727-753.
[40] D. Feng, Z. Zhao, P. Li, Y. Li, J. Zha, J. Hu, Y. Zhang, Y. Feng, Multifunctional performance of carbon nanotubes in thermal energy storage materials, Materials Today 75 (2024) 285-308.
[41] L. Hu, L. Zhang, W. Cui, Q. An, T. Ma, Q. Wang, L. Mai, Carbon-based porous materials for performance-enhanced composite phase change materials in thermal energy storage: Materials, fabrication and applications, Journal of Materials Science & Technology 210 (2025) 204-226.
[42] Q. Zhu, P.J. Ong, S.H.A. Goh, R.J. Yeo, S. Wang, Z. Liu, X.J. Loh, Recent advances in graphene-based phase change composites for thermal energy storage and management, Nano Materials Science 6(2) (2024) 115-138.
[43] C. Zhao, X. He, N. Sheng, C. Zhu, Directional fiber framework wrapped by graphene flakes for supporting phase change material with fast thermal energy storage properties, Journal of Energy Storage 57 (2023) 106304.

[44] H. Zhu, M. Gu, X. Dai, S. Feng, T. Yang, Y. Fan, J. Zhang, D. Fan, Y. Liu, Y. Lu, P. Zhu, H. Lu, T. Qian, Y. Cao, C. Yan, Mechanically strong, healable, and recyclable supramolecular solid–solid phase change materials with high thermal conductivity for thermal energy storage, Chemical Engineering Journal 494 (2024) 153235.
[45] A. Vinod, H. Pulikkalparambil, P. Jagadeesh, S.M. Rangappa, S. Siengchin, Recent advancements in lignocellulose biomass-based carbon fiber: Synthesis, properties, and applications, Heliyon 9(3) (2023).
[46] M.M. Umair, Y. Zhang, K. Iqbal, S. Zhang, B. Tang, Novel strategies and supporting materials applied to shape-stabilize organic phase change materials for thermal energy storage–A review, Applied Energy 235 (2019) 846-873.
[47] H. He, R. Zhang, P. Zhang, P. Wang, N. Chen, B. Qian, L. Zhang, J. Yu, B. Dai, Functional carbon from nature: biomass-derived carbon materials and the recent progress of their applications, Advanced Science 10(16) (2023) 2205557.
[48] K. Liu, Z. Yuan, H. Zhao, C. Shi, F. Zhao, Properties and applications of shape-stabilized phase change energy storage materials based on porous material support—A review, Materials Today Sustainability 21 (2023) 100336.
[49] X. Yang, H. He, T. Lv, J. Qiu, Fabrication of biomass-based functional carbon materials for energy conversion and storage, Materials Science and Engineering: R: Reports 154 (2023) 100736.
[50] M. Wu, J. Liao, L. Yu, R. Lv, P. Li, W. Sun, R. Tan, X. Duan, L. Zhang, F. Li, 2020 Roadmap on carbon materials for energy storage and conversion, Chemistry–An Asian Journal 15(7) (2020) 995-1013.
[51] J. Song, H. He, Y. Wang, L. Shao, Q. Wang, Q. Wei, Y. Cai, Shape-stabilized phase change composites supported by biomass loofah sponge-derived microtubular carbon scaffold toward thermal energy storage and electric-to-thermal conversion, Journal of Energy Storage 56 (2022) 105891.
[52] N. Sheng, Z. Rao, C. Zhu, H. Habazaki, Enhanced thermal performance of phase change material stabilized with textile-structured carbon scaffolds, Solar Energy Materials and Solar Cells 205 (2020) 110241.
[53] T. Jiang, Y. Zhang, S. Olayiwola, C. Lau, M. Fan, K. Ng, G. Tan, Biomass-derived porous carbons support in phase change materials for building energy efficiency: a review, Materials Today Energy 23 (2022) 100905.
[54] Y. Luo, F. Zhang, C. Li, J. Cai, Biomass-based shape-stable phase change materials supported by garlic peel-derived porous carbon for thermal energy storage, Journal of Energy Storage 46 (2022) 103929.
[55] X.Y. Soo, J.K. Muiruri, J.C. Yeo, Z.M. Png, A. Sng, H. Xie, R. Ji, S. Wang, H. Liu, J. Xu, Polyethylene glycol/polylactic acid block co-polymers as solid–solid phase change materials, SmartMat 4(3) (2023) e1188.
[56] P.J. Ong, S.H.A. Goh, Y. Leow, S. Wang, P. Wang, Z. Li, X. Yin, B.H. Tan, W. Thitsartarn, J. Xu, Valorization of coconut peat to develop a novel shape-stabilized phase change material for thermal energy storage, Journal of Cleaner Production (2024) 141468.
[57] M.T. Hossain, M.A. Shahid, M.Y. Ali, S. Saha, M.S.I. Jamal, A. Habib, Fabrications, Classifications, and Environmental Impact of PCM-Incorporated Textiles: Current State and Future Outlook, ACS Omega 8(48) (2023) 45164-45176.
[58] L. Lv, S. Huang, H. Zhou, Effect of introducing chemically activated biochar as support material on thermal properties of different organic phase change materials, Solar Energy Materials and Solar Cells 264 (2024) 112617.
[59] D. Li, H. Sun, T. Li, M. Yang, T. Xiong, D. Sun, Enhanced thermal conductivity of a superhydrophobic thermal energy storage coating based on artificially cultured diatom frustules, Applied Energy 347 (2023) 121462.

[60] H. Sun, T. Li, L. Sha, F. Chen, M. Li, Y. Yang, B. Li, D. Li, D. Sun, Comparative of diatom frustules, diatomite, and silica particles for constructing self-healing superhydrophobic materials with capacity for thermal energy storage, Applied Energy 332 (2023) 120482.
[61] H. Maeda, M. Matsumoto, Y. Maeda, Y. Egashira, T. Tanaka, T. Kasuga, Utilization of diatom frustules for thermal management applications, Journal of Applied Phycology 29 (2017) 1907-1911.
[62] J. Huang, B. Wu, S. Lyu, T. Li, H. Han, D. Li, J.-K. Wang, J. Zhang, X. Lu, D. Sun, Improving the thermal energy storage capability of diatom-based biomass/polyethylene glycol composites phase change materials by artificial culture methods, Solar Energy Materials and Solar Cells 219 (2021) 110797.
[63] B. Wu, S. Lyu, H. Han, T. Li, H. Sun, J.-K. Wang, D. Li, F. Lei, J. Huang, D. Sun, Biomass-based shape-stabilized phase change materials from artificially cultured ship-shaped diatom frustules with high enthalpy for thermal energy storage, Composites Part B: Engineering 205 (2021) 108500.
[64] X.W. Sun, Y.X. Zhang, D. Losic, Diatom silica, an emerging biomaterial for energy conversion and storage, Journal of Materials Chemistry A 5(19) (2017) 8847-8859.
[65] X.Y.D. Soo, Z.M. Png, X. Wang, M.H. Chua, P.J. Ong, S. Wang, Z. Li, D. Chi, J. Xu, X.J. Loh, Rapid UV-curable form-stable polyethylene-glycol-based phase change material, ACS Applied Polymer Materials 4(4) (2022) 2747-2756.
[66] W.-Y. Wu, I.S.R. Yeap, S. Wang, N. Tomczak, M. Lin, D. Kai, E. Ye, W. Thitsartarn, J.B.H. Tan, X. Yin, Advancements in sustainable phase change materials: Valorizing waste for eco-friendly applications, Materials Today Chemistry 39 (2024) 102163.
[67] W.-Y. Wu, M. Gao, R.Y. Jueyuan, M. Lin, S. Wang, W. Thitsartarn, X. Zhang, D. Kai, P. Wang, Z. Qu, Plant oil-based phase change materials for sustainable thermal energy storage: A review, Fuel 378 (2024) 132940.
[68] B.K. Purohit, V.S. Sistla, Inorganic salt hydrate for thermal energy storage application: A review, Energy Storage 3(2) (2021) e212.
[69] M. Li, B. Mu, Effect of different dimensional carbon materials on the properties and application of phase change materials: A review, Applied Energy 242 (2019) 695-715.
[70] R.K. Mishra, K. Verma, V. Mishra, B. Chaudhary, A review on carbon-based phase change materials for thermal energy storage, Journal of Energy Storage 50 (2022) 104166.
[71] J. Zheng, S.F.D. Solco, C.J.E. Wong, S.A. Sia, X.Y. Tan, J. Cao, J.C.C. Yeo, W. Yan, Q. Zhu, Q. Yan, Integrating recyclable polymers into thermoelectric devices for green electronics, Journal of Materials Chemistry A 10(37) (2022) 19787-19796.
[72] Q. Zhu, E. Yildirim, X. Wang, A.K.K. Kyaw, T. Tang, X.Y.D. Soo, Z.M. Wong, G. Wu, S.-W. Yang, J. Xu, Effect of substituents in sulfoxides on the enhancement of thermoelectric properties of PEDOT: PSS: experimental and modelling evidence, Molecular Systems Design & Engineering 5(5) (2020) 976-984.
[73] W.-Y. Wu, M. Zhang, C. Wang, L. Tao, J. Bu, Q. Zhu, Harnessing Ash for Sustainable CO2 Absorption: Current Strategies and Future Prospects, Chemistry–An Asian Journal (2024) e202400180.
[74] X.Y.D. Soo, J.J.C. Lee, W.-Y. Wu, L. Tao, C. Wang, Q. Zhu, J. Bu, Advancements in CO2 capture by absorption and adsorption: A comprehensive review, Journal of CO2 Utilization 81 (2024) 102727.
[75] E. Yildirim, Q. Zhu, G. Wu, T.L. Tan, J. Xu, S.-W. Yang, Self-organization of PEDOT: PSS induced by green and water-soluble organic molecules, The Journal of Physical Chemistry C 123(15) (2019) 9745-9755.
[76] J. Cao, S.W. Chien, X.Y. Tan, C.K.I. Tan, Q. Zhu, J. Wu, X. Wang, Y. Zhao, L. Yang, Q. Yan, Realizing zT values of 2.0 in cubic GeTe, ChemNanoMat 7(4) (2021) 476-482.

[77] R.J. Yeo, A. Sng, C. Wang, L. Tao, Q. Zhu, J. Bu, Strategies for heavy metals immobilization in municipal solid waste incineration bottom ash: a critical review, Reviews in Environmental Science and Bio/Technology (2024) 1-66.
[78] K. Zhou, Y. Sheng, W. Guo, L. Wu, H. Wu, X. Hu, Y. Xu, Y. Li, M. Ge, Y. Du, Biomass porous carbon/polyethylene glycol shape-stable phase change composites for multi-source driven thermal energy conversion and storage, Advanced Composites and Hybrid Materials 6(1) (2023) 34.
[79] Y. Chen, Y. Meng, J. Zhang, Y. Xie, H. Guo, M. He, X. Shi, Y. Mei, X. Sheng, D. Xie, Leakage Proof, Flame-Retardant, and Electromagnetic Shield Wood Morphology Genetic Composite Phase Change Materials for Solar Thermal Energy Harvesting, Nano-Micro Letters 16(1) (2024) 196.
[80] J. Nam, B.Y. Yun, J.Y. Choi, S. Kim, Potential of wood as thermal energy storage materials: Different characteristics depending on the hierarchical structure and components, International Journal of Energy Research 46(11) (2022) 14926-14945.
[81] H. Chen, J. Xuan, Q. Deng, Y. Gao, WOOD/PCM composite with enhanced energy storage density and anisotropic thermal conductivity, Progress in Natural Science: Materials International 32(2) (2022) 190-195.
[82] C. Qi, F. Zhang, J. Mu, Y. Zhang, Z. Yu, Enhanced mechanical and thermal properties of hollow wood composites filled with phase-change material, Journal of Cleaner Production 256 (2020) 120373.
[83] R. Xia, W. Zhang, Y. Yang, J. Zhao, Y. Liu, H. Guo, Transparent wood with phase change heat storage as novel green energy storage composites for building energy conservation, Journal of Cleaner Production 296 (2021) 126598.
[84] A.M. Mohammed, A. Elnokaly, A.M.M. Aly, Empirical investigation to explore potential gains from the amalgamation of phase changing materials (PCMs) and wood shavings, Energy and Built Environment 2(3) (2021) 315-326.
[85] M. Zhou, J. Wang, Y. Zhao, G. Wang, W. Gu, G. Ji, Hierarchically porous wood-derived carbon scaffold embedded phase change materials for integrated thermal energy management, electromagnetic interference shielding and multifunctional application, Carbon 183 (2021) 515-524.
[86] F. Hanif, M. Imran, Y. Zhang, Z. Jia, X. Lu, R. Lu, B. Tang, Form-Stable Phase Change Material with Wood-Based Materials as Support, Polymers 15(4) (2023) 942.
[87] H. Saavedra, C. García-Herrera, D.A. Vasco, C. Salinas-Lira, Characterization of mechanical performance of Pinus radiata wood impregnated with octadecane as phase change material, Journal of Building Engineering 34 (2021) 101913.
[88] R. Fuentes-Sepúlveda, C. García-Herrera, D.A. Vasco, C. Salinas-Lira, R.A. Ananías, Thermal Characterization of Pinus radiata Wood Vacuum-Impregnated with Octadecane, Energies 13(4) (2020) 942.
[89] B. Liang, X. Lu, R. Li, W. Tu, Z. Yang, T. Yuan, Solvent-free preparation of bio-based polyethylene glycol/wood flour composites as novel shape-stabilized phase change materials for solar thermal energy storage, Solar Energy Materials and Solar Cells 200 (2019) 110037.
[90] P.J. Ong, Y.Y. Lum, X.Y.D. Soo, S. Wang, P. Wang, D. Chi, H. Liu, D. Kai, C.-L.K. Lee, Q. Yan, Integration of phase change material and thermal insulation material as a passive strategy for building cooling in the tropics, Construction and Building Materials 386 (2023) 131583.
[91] V. Bui, H. Liu, Y. Low, T. Tang, Q. Zhu, K. Shah, E. Shidoji, Y. Lim, W. Koh, Evaluation of building glass performance metrics for the tropical climate, Energy and Buildings 157 (2017) 195-203.

[92] Z.M. Png, X.Y.D. Soo, M.H. Chua, P.J. Ong, J. Xu, Q. Zhu, Triazine derivatives as organic phase change materials with inherently low flammability, Journal of Materials Chemistry A 10(7) (2022) 3633-3641.
[93] J. Zhao, Y. Li, X. Fang, J. Sun, W. Zhang, B. Wang, J. Xu, Y. Liu, H. Guo, High interface compatibility and phase change enthalpy of heat storage wood plastic composites as bio-based building materials for energy saving, Journal of Energy Storage 51 (2022) 104293.
[94] L. Ma, Q. Wang, L. Li, Delignified wood/capric acid-palmitic acid mixture stable-form phase change material for thermal storage, Solar Energy Materials and Solar Cells 194 (2019) 215-221.
[95] Y. Sun, N. Zhang, X. Pan, W. Zhong, B. Qiu, Y. Cai, Y. Yuan, Thermal properties of biomass-based form-stable phase change material for latent heat thermal energy storage, International Journal of Energy Research 45(14) (2021) 20372-20383.
[96] W.Y. Wu, G.M.D. Yeo, S. Wang, Z. Liu, X.J. Loh, Q. Zhu, Recent Progress in Polyethylene-enhanced Organic Phase Change Composite Materials for Energy Management, Chemistry–An Asian Journal 18(14) (2023) e202300391.
[97] J.J.C. Lee, N.N.A. Hayat, X.Y.D. Soo, S.Y. Tan, Y.Y.K. Hnin, S. Wang, F. Wei, D. Kai, F. Wang, P. Luo, Upcycling of PET plastics into diethyl terephthalate for applications as phase change materials in energy harvesting, Journal of Energy Storage 73 (2023) 109084.
[98] P.J. Ong, Z.M. Png, X.Y.D. Soo, X. Wang, A. Suwardi, M.H. Chua, J.W. Xu, Q. Zhu, Surface modification of microencapsulated phase change materials with nanostructures for enhancement of their thermal conductivity, Materials Chemistry and Physics 277 (2022) 125438.
[99] Y. Meng, J. Majoinen, B. Zhao, O.J. Rojas, Form-stable phase change materials from mesoporous balsa after selective removal of lignin, Composites Part B: Engineering 199 (2020) 108296.
[100] J. Zhang, Y. Xu, X. Li, H. Li, C. Yao, S. Chen, F. Xu, Leak-free, high latent heat and self-cleaning phase change materials supported by layered cellulose/Fe3O4 skeleton for light-to-thermal energy conversion, Energy Conversion and Management 256 (2022) 115357.
[101] X. Pan, N. Zhang, Y. Yuan, X. Shao, W. Zhong, L. Yang, Balsa-based porous carbon composite phase change material with photo-thermal conversion performance for thermal energy storage, Solar Energy 230 (2021) 269-277.
[102] X. Li, Z. Zhu, P. Yang, Z. You, Y. Dong, M. Tang, M. Chen, X. Zhou, Carbonized wood loaded with carbon dots for preparation long-term shape-stabilized composite phase change materials with superior thermal energy conversion capacity, Renewable Energy 174 (2021) 19-30.
[103] Y.-c. Wan, Y. Chen, Z.-x. Cui, H. Ding, S.-f. Gao, Z. Han, J.-k. Gao, A promising form-stable phase change material prepared using cost effective pinecone biochar as the matrix of palmitic acid for thermal energy storage, Scientific Reports 9(1) (2019) 11535.
[104] N. Feng, Z. Kang, D. Hu, Shape-stabilized and antibacterial composite phase change materials based on wood-based cellulose micro-framework, erythritol-urea or erythritol-thiourea for thermal energy storage, Solar Energy 223 (2021) 19-32.
[105] M.A. Fikri, A.K. Pandey, M. Samykano, K. Kadirgama, M. George, R. Saidur, J. Selvaraj, N.A. Rahim, K. Sharma, V.V. Tyagi, Thermal conductivity, reliability, and stability assessment of phase change material (PCM) doped with functionalized multi-wall carbon nanotubes (FMWCNTs), Journal of Energy Storage 50 (2022) 104676.
[106] S.P. Chitriv, K. Dharmadhikari, N. A ．, A.S. Archak, V. R ．P ．, G.C. Dsouza, Unzipped multiwalled carbon nanotube oxide / PEG based phase change composite for latent heat energy storage, International Journal of Heat and Mass Transfer 220 (2024) 124908.

[107] L. Cao, D. Zhang, Application potential of graphene aerogel in paraffin phase change composites: Experimental study and guidance based on numerical simulation, Solar Energy Materials and Solar Cells 223 (2021) 110949.
[108] F. Cheng, Z. Lv, Y. Xu, Z. Huang, X. Min, M. Fang, Y.g. Liu, X. Wu, A novel function-designed carbon fiber reinforced polymer with implanting expanded graphite/paraffin composite into interlayers: Mechanical, thermal and sustainable properties analysis, Composites Science and Technology 188 (2020) 107965.
[109] C.O. Chin, X. Yang, S.C. Paul, Susilawati, L.S. Wong, S.Y. Kong, Development of thermal energy storage lightweight concrete using paraffin-oil palm kernel shell-activated carbon composite, Journal of Cleaner Production 261 (2020) 121227.
[110] X. Zhu, Q. Wang, S. Kang, J. Li, X. Jia, Coal-based ultrathin-wall graphitic porous carbon for high-performance form-stable phase change materials with enhanced thermal conductivity, Chemical Engineering Journal 395 (2020) 125112.
[111] X.Y.D. Soo, L. Jia, Q.F. Lim, M.H. Chua, S. Wang, H.K. Hui, J.M.R. See, Y. Chen, J. Li, F. Wei, Hydrolytic degradation and biodegradation of polylactic acid electrospun fibers, Chemosphere 350 (2024) 141186.
[112] J.K. Muiruri, J.C. Chuan Yeo, Q. Zhu, E. Ye, X.J. Loh, Z. Li, Sustainable mycelium-bound biocomposites: design strategies, materials properties, and emerging applications, ACS Sustainable Chemistry & Engineering 11(18) (2023) 6801-6821.
[113] X.Y.D. Soo, J.K. Muiruri, W.Y. Wu, J.C.C. Yeo, S. Wang, N. Tomczak, W. Thitsartarn, B.H. Tan, P. Wang, F. Wei, Bio-Polyethylene and Polyethylene Biocomposites: An Alternative toward a Sustainable Future, Macromolecular Rapid Communications (2024) 2400064.
[114] J.K. Muiruri, J.C.C. Yeo, X.Y.D. Soo, S. Wang, H. Liu, J. Kong, J. Cao, B.H. Tan, A. Suwardi, Z. Li, Recent advances of sustainable Short-chain length polyhydroxyalkanoates (Scl-PHAs)–Plant biomass composites, European Polymer Journal 187 (2023) 111882.
[115] X. Wang, L. Hu, Turning powders into fibre via cellulose, Nature Materials 23(5) (2024) 579-580.
[116] H. Wang, C. Zeng, C. Wang, J. Fu, Y. Li, Y. Yang, Z. Du, G. Tao, Q. Sun, T. Zhai, H. Li, Fibration of powdery materials, Nature Materials 23(5) (2024) 596-603.
[117] S. Wang, P.J. Ong, S. Liu, W. Thitsartarn, M.J.B.H. Tan, A. Suwardi, Q. Zhu, X.J. Loh, Recent advances in host-guest supramolecular hydrogels for biomedical applications, Chemistry–An Asian Journal 17(18) (2022) e202200608.
[118] H. Zhu, J.M.J. Qiang, C.G. Wang, C.Y. Chan, Q. Zhu, E. Ye, Z. Li, X.J. Loh, Flexible polymeric patch based nanotherapeutics against non-cancer therapy, Bioactive Materials 18 (2022) 471-491.
[119] M. Liu, Y. Chen, Q. Zhu, J. Tao, C. Tang, H. Ruan, Y. Wu, X.J. Loh, Antioxidant thermogelling formulation for burn wound healing, Chemistry–An Asian Journal 17(16) (2022) e202200396.
[120] J. Chen, Y. Zhang, F. Wu, B. Guan, X. Du, H. Wang, Cellulose nanofiber/melanin hybrid aerogel supported phase change materials with improved photothermal conversion efficiency and superior energy storage density, Cellulose 28(15) (2021) 9739-9750.
[121] X. Du, J. Qiu, S. Deng, Z. Du, X. Cheng, H. Wang, Alkylated Nanofibrillated Cellulose/Carbon Nanotubes Aerogels Supported Form-Stable Phase Change Composites with Improved n-Alkanes Loading Capacity and Thermal Conductivity, ACS Applied Materials & Interfaces 12(5) (2020) 5695-5703.
[122] Y. Tan, X. Du, Z. Du, H. Wang, X. Cheng, Form-stable phase change composites based on nanofibrillated cellulose/polydopamine hybrid aerogels with extremely high energy storage density and improved photothermal conversion efficiency, RSC Advances 11(10) (2021) 5712-5721.

[123] X. Du, M. Zhou, S. Deng, Z. Du, X. Cheng, H. Wang, Poly(ethylene glycol)-grafted nanofibrillated cellulose/graphene hybrid aerogels supported phase change composites with superior energy storage capacity and solar-thermal conversion efficiency, Cellulose 27(8) (2020) 4679-4690.
[124] X. Du, J. Qiu, S. Deng, Z. Du, X. Cheng, H. Wang, Flame-retardant and form-stable phase change composites based on black phosphorus nanosheets/cellulose nanofiber aerogels with extremely high energy storage density and superior solar-thermal conversion efficiency, Journal of Materials Chemistry A 8(28) (2020) 14126-14134.
[125] T. Tang, A.K.K. Kyaw, Q. Zhu, J. Xu, Water-dispersible conducting polyazulene and its application in thermoelectrics, Chemical Communications 56(65) (2020) 9388-9391.
[126] T.A. Yemata, A.K.K. Kyaw, Y. Zheng, X. Wang, Q. Zhu, W.S. Chin, J. Xu, Enhanced thermoelectric performance of poly (3, 4-ethylenedioxythiophene): poly (4-styrenesulfonate)(PEDOT: PSS) with long-term humidity stability via sequential treatment with trifluoroacetic acid, Polymer International 69(1) (2020) 84-92.
[127] J. Cao, J. Zheng, H. Liu, C.K.I. Tan, X. Wang, W. Wang, Q. Zhu, Z. Li, G. Zhang, J. Wu, Flexible elemental thermoelectrics with ultra-high power density, Materials Today Energy 25 (2022) 100964.
[128] J. Dong, A. Suwardi, X.Y. Tan, N. Jia, K. Saglik, R. Ji, X. Wang, Q. Zhu, J. Xu, Q. Yan, Challenges and opportunities in low-dimensional thermoelectric nanomaterials, Materials Today (2023).
[129] F. Wei, B. Cheng, L.T. Chew, J.J. Lee, K.H. Cheong, J. Wu, Q. Zhu, C.C. Tan, Grain distribution characteristics and effect of diverse size distribution on the Hall–Petch relationship for additively manufactured metal alloys, Journal of Materials Research and Technology 20 (2022) 4130-4136.
[130] A. Sarcinella, M. Frigione, Selection of PEG-Matrix Combinations to Achieve High Performance Form-Stable Phase Change Materials for Building Applications, Coatings 14(3) (2024) 250.
[131] N. Sheng, T. Nomura, C. Zhu, H. Habazaki, T. Akiyama, Cotton-derived carbon sponge as support for form-stabilized composite phase change materials with enhanced thermal conductivity, Solar Energy Materials and Solar Cells 192 (2019) 8-15.
[132] N. Sheng, R. Zhu, T. Nomura, Z. Rao, C. Zhu, Y. Aoki, H. Habazaki, T. Akiyama, Anisotropically enhanced heat transfer properties of phase change material reinforced by graphene-wrapped carbon fibers, Solar Energy Materials and Solar Cells 206 (2020) 110280.
[133] H. Bi, H. Huang, F. Xu, T. Lin, H. Zhang, F. Huang, Carbon microtube/graphene hybrid structures for thermal management applications, Journal of Materials Chemistry A 3(36) (2015) 18706-18710.
[134] M.M. Umair, Y. Zhang, A. Tehrim, S. Zhang, B. Tang, Form-Stable Phase-Change Composites Supported by a Biomass-Derived Carbon Scaffold with Multiple Energy Conversion Abilities, Industrial & Engineering Chemistry Research 59(4) (2020) 1393-1401.
[135] R.J. Yeo, J.C. Yeo, S. Yu Tan, A. Sng, N. Tomczak, J.K. Muiruri, S. Wang, P. Wang, W. Thitsartarn, F. Wang, Core-Shell Micro-and Nano-Structures for The Modification of Light-Surface Interactions, Advanced Optical Materials 12(4) (2024) 2301955.
[136] R. Yeo, W.-Y. Wu, N. Tomczak, R. Ji, S. Wang, X. Wang, J. Kong, H. Liu, K. Goh, J. Xu, Tailoring surface reflectance through nanostructured materials design for energy-efficient applications, Materials Today Chemistry 30 (2023) 101593.
[137] J. Wu, S. Wang, R. Ji, D. Kai, J. Kong, S. Liu, W. Thitsartarn, B.H. Tan, M.H. Chua, J. Xu, In Situ Characterization Techniques for Electrochemical Nitrogen Reduction Reaction, ACS nano (2024).

[138] C. Zhu, C. Zhao, Z. Chen, R. Zhu, N. Sheng, Z. Rao, Anisotropically thermal transfer improvement and shape stabilization of paraffin supported by SiC-coated biomass carbon fiber scaffolds for thermal energy storage, Journal of Energy Storage 46 (2022) 103866.
[139] N. Sheng, Z. Rao, C. Zhu, H. Habazaki, Honeycomb carbon fibers strengthened composite phase change materials for superior thermal energy storage, Applied Thermal Engineering 164 (2020) 114493.
[140] M. Sun, F. Sun, H. Di, C. Wu, H. Sheng, L. Lin, Q. Wang, High value utilization of waste peanut shell: Prepared novel shape stable composite phase change materials with high thermal conductivity, Materials Today Sustainability 26 (2024) 100707.
[141] Y. Chen, Z. Cui, H. Ding, Y. Wan, Z. Tang, J. Gao, Cost-Effective Biochar Produced from Agricultural Residues and Its Application for Preparation of High Performance Form-Stable Phase Change Material via Simple Method, International Journal of Molecular Sciences 19(10) (2018) 3055.
[142] Y. Xie, S. Xiao, W. Chen, X. Hu, Y. Liu, L. Jiang, L. Luo, W. Luo, Y. Ma, X. Jiang, Y. He, Q. Li, Shape-stabilized nanosilver-modified grapefruit peel-based porous carbon composite phase change material with high thermal conductivity, photothermal conversion performance and thermal management capability, Journal of Energy Storage 83 (2024) 110819.
[143] J.Y. Choi, J. Nam, H. Yuk, S. Yang, S. Kim, Enhancing the hygrothermal performance of corn cob residue-based eco-friendly building materials through biochar and microencapsulated phase change material incorporation, Journal of Building Engineering 89 (2024) 109189.
[144] P. Kumar, S. Thomas, C.B. Sobhan, G.P. Peterson, Activated carbon foam composite derived from PEG400/ Terminalia Catappa as form stable PCM for sub-zero cold energy storage, Journal of Cleaner Production 434 (2024) 139993.
[145] Q. Zhu, Y. Lu, Chiral amine-mediated asymmetric conjugate additions to vinyl sulfones, Australian journal of chemistry 62(9) (2009) 951-955.
[146] J. Gao, Q. Xu, J. Zhang, S. Wu, Y. Chen, Q. Shi, Fabrication of a Novel Highly Thermal Conductive Shape-Stabilized Phase-Change Material Using Cheap and Easily Available Cabbage Mustard Biochar as the Matrix, JOM 73(8) (2021) 2487-2494.
[147] Z. Zou, W. Wu, W. Shen, Introduction of Phase Change Material into Sustainable Carbon Materials for Enhanced Shape Stability and Thermal Conductivity, ChemistrySelect 5(28) (2020) 8679-8686.
[148] Z. Zou, W. Wu, Y. Wang, D. Drummer, Biomass derived carbon aerogel as an ultrastable skeleton of form-stable phase change materials for efficient thermal energy storage, Materials Research Express 7(4) (2020) 045601.
[149] P. Jin Ong, Y. Leow, X. Yun Debbie Soo, M. Hui Chua, X. Ni, A. Suwardi, C. Kiang Ivan Tan, R. Zheng, F. Wei, J. Xu, X. Jun Loh, D. Kai, Q. Zhu, Valorization of Spent coffee Grounds: A sustainable resource for Bio-based phase change materials for thermal energy storage, Waste Management 157 (2023) 339-347.
[150] J. Yoo, S.J. Chang, S. Wi, S. Kim, Spent coffee grounds as supporting materials to produce bio-composite PCM with natural waxes, Chemosphere 235 (2019) 626-635.
[151] X. Hu, H. Huang, Y. Hu, X. Lu, Y. Qin, Novel bio-based composite phase change materials with reduced graphene oxide-functionalized spent coffee grounds for efficient solar-to-thermal energy storage, Solar Energy Materials and Solar Cells 219 (2021) 110790.
[152] W. Zhang, X. Zhang, X. Zhang, Z. Yin, Y. Liu, M. Fang, X. Wu, X. Min, Z. Huang, Lauric-stearic acid eutectic mixture/carbonized biomass waste corn cob composite phase change materials: Preparation and thermal characterization, Thermochimica Acta 674 (2019) 21-27.
[153] R. Wen, Y. Liu, C. Yang, X. Zhu, Z. Huang, X. Zhang, W. Gao, Enhanced thermal properties of stearic acid/carbonized maize straw composite phase change material for thermal energy storage in buildings, Journal of Energy Storage 36 (2021) 102420.

[154] Y. Li, X. Huang, Y. Li, Z. Xi, G. Hai, Z. Tao, G. Wang, Shape-stabilized phase-change materials supported by eggplant-derived porous carbon for efficient solar-to-thermal energy conversion and storage, Sustainable Energy & Fuels 4(4) (2020) 1764-1772.
[155] C. Zhang, X. Hu, S. Xiao, W. Luo, H. Wang, X. Jiang, Enhanced thermal performance of phase-change material supported by nano-Ag coated eggplant-based biological porous carbon, Journal of Energy Storage 43 (2021) 103174.
[156] K. Yu, Y. Liu, M. Jia, Y. Yang, Bio-Based Dual-Functionalized Phase Change Composite: Ultrafast Solar-to-Thermal Conversion and Reinforced Heat Storage Capacity, Energy & Fuels 35(19) (2021) 16162-16173.
[157] H. Liu, Z. Zheng, Z. Qian, Q. Wang, D. Wu, X. Wang, Lamellar-structured phase change composites based on biomass-derived carbonaceous sheets and sodium acetate trihydrate for high-efficient solar photothermal energy harvest, Solar Energy Materials and Solar Cells 229 (2021) 111140.
[158] H. Liu, Z. Qian, Q. Wang, D. Wu, X. Wang, Development of Renewable Biomass-Derived Carbonaceous Aerogel/Mannitol Phase-Change Composites for High Thermal-Energy-Release Efficiency and Shape Stabilization, ACS Applied Energy Materials 4(2) (2021) 1714-1730.
[159] K. Sun, Y. Kou, Y. Zhang, T. Liu, Q. Shi, Photo-triggered Hierarchical Porous Carbon-Based Composite Phase-Change Materials with Superior Thermal Energy Conversion Capacity, ACS Sustainable Chemistry & Engineering 8(8) (2020) 3445-3453.
[160] M.A. Tony, From biomass residue to solar thermal energy: the potential of bagasse as a heat storage material, Euro-Mediterranean Journal for Environmental Integration 5(1) (2020) 17.
[161] J. Su, M. Weng, X. Lu, W. Xu, S. Lyu, Y. Liu, Y. Min, Functional Unit Construction for Heat Storage by Using Biomass-Based Composite, Frontiers in Chemistry 10 (2022) 835455.
[162] Z. Yu, X. Li, J. Wang, S. Zhang, Form-stable Na2CO3-NaCl/mullite phase change composite with SiC enhanced thermal conductivity for high temperature thermal storage, Journal of Energy Storage 87 (2024) 111511.
[163] Z. Geng, C. Shi, Q. Zhao, L. Yang, Preparation of diatomite paraffin composite phase change coating and its simulation application in building wall, Journal of Energy Storage 83 (2024) 110543.
[164] C. Li, L. Han, Q. Li, G. Leng, H. Lu, R. Xu, Y. Du, Y. Wu, Development and investigation of salt based composite phase change material containing diatomite as skeleton substance by cold sintering technology for medium and high temperature thermal energy storage, Solar Energy Materials and Solar Cells 271 (2024) 112821.
[165] T. Fu, W. Wang, G. Fang, Thermal properties and applications of form-stable phase change materials for thermal energy storage and thermal management: A review, Energy Storage 6(1) (2024) e533.
[166] S. Wang, J.K. Muiruri, X.Y.D. Soo, S. Liu, W. Thitsartarn, B.H. Tan, A. Suwardi, Z. Li, Q. Zhu, X.J. Loh, Bio-Polypropylene and Polypropylene-based Biocomposites: Solutions for a Sustainable Future, Chemistry–An Asian Journal 18(2) (2023) e202200972.
[167] Z.M. Png, C.-G. Wang, J.C.C. Yeo, J.J.C. Lee, N.E. Surat'man, Y.L. Tan, H. Liu, P. Wang, B.H. Tan, J.W. Xu, Stimuli-responsive structure–property switchable polymer materials, Molecular Systems Design & Engineering 8(9) (2023) 1097-1129.
[168] M.H. Chua, S.H.G. Toh, P.J. Ong, Z.M. Png, Q. Zhu, S. Xiong, J. Xu, Towards modulating the colour hues of isoindigo-based electrochromic polymers through variation of thiophene-based donor groups, Polymer Chemistry 13(7) (2022) 967-981.
[169] X.Y.D. Soo, D. Zhang, S.Y. Tan, Y.T. Chong, H.K. Hui, A. Sng, F. Wei, A. Suwardi, Z.M. Png, Q. Zhu, Ultra-high Performance Thermochromic Polymers via a Solid-solid Phase Transition Mechanism and Their Applications, Advanced Materials (2024) 2405430.

[170] H. Sun, T. Li, F. Lei, S. Lyu, Y. Yang, B. Li, H. Han, B. Wu, J. Huang, C. Zhang, D. Li, D. Sun, Fast Self-Healing Superhydrophobic Thermal Energy Storage Coatings Fabricated by Bio-Based Beeswax and Artificially Cultivated Diatom Frustules, ACS Applied Materials & Interfaces 13(40) (2021) 48088-48100.
[171] J.Y. Choi, Y.U. Kim, J. Nam, S. Kim, S. Kim, Enhancing the thermal stability and fire retardancy of bio-based building materials through pre-biochar system, Construction and Building Materials 409 (2023) 134099.
[172] P. B, V.A. A, S. Nižetić, M. Arıcı, R. Nallamuthu, A comprehensive assessment on biomass derived form-stabilized composite phase change materials for solar thermal energy storage systems, Journal of Energy Storage 86 (2024) 111278.
[173] L. He, H. Jing, Y. Zhang, P. Li, Z. Gu, Review of thermal management system for battery electric vehicle, Journal of Energy Storage 59 (2023) 106443.
[174] U. Bordoloi, D. Das, D. Kashyap, D. Patwa, P. Bora, H.H. Muigai, P. Kalita, Synthesis and comparative analysis of biochar based form-stable phase change materials for thermal management of buildings, Journal of Energy Storage 55 (2022) 105801.
[175] D. Gowthami, R.K. Sharma, V.V. Tyagi, P.K.S. Rathore, A. Sarı, Development of a novel form-stable phase change material based on alkali activated date seed biochar to harvest solar thermal energy, Journal of Energy Storage 83 (2024) 110699.
[176] Y.U. Kim, B.Y. Yun, J. Nam, J.Y. Choi, S. Wi, S. Kim, Evaluation of thermal properties of phase change material-integrated artificial stone according to biochar loading content, Construction and Building Materials 305 (2021) 124682.
[177] C. Li, Z. Sun, Y. Wang, J. Zhu, J. Wu, L. Feng, X. Wen, W. Cai, H. Yu, M. Wang, J. Wu, D. Liu, A novel biogenic porous core/shell-based shape-stabilized phase change material for building energy saving, Journal of Energy Storage 95 (2024) 112504.
[178] C. Li, X. Wen, W. Cai, H. Yu, D. Liu, Phase change material for passive cooling in building envelopes: A comprehensive review, Journal of Building Engineering 65 (2023) 105763.
[179] H. Yu, C. Li, K. Zhang, Y. Tang, Y. Song, M. Wang, Preparation and thermophysical performance of diatomite-based composite PCM wallboard for thermal energy storage in buildings, Journal of Building Engineering 32 (2020) 101753.
[180] D. Das, O. Masek, M.C. Paul, Development of novel form-stable PCM-biochar composites and detailed characterization of their morphological, chemical and thermal properties, Journal of Energy Storage 84 (2024) 110995.
[181] J. Wang, Y. Wang, R. Yang, Flame retardance property of shape-stabilized phase change materials, Solar Energy Materials and Solar Cells 140 (2015) 439-445.
[182] C. Li, H. Yu, Y. Song, M. Wang, Z. Liu, A n-octadecane/hierarchically porous TiO2 form-stable PCM for thermal energy storage, Renewable Energy 145 (2020) 1465-1473.
[183] J. Cheng, S. Niu, M. Kang, Y. Liu, F. Zhang, W. Qu, Y. Guan, S. Li, The thermal behavior and flame retardant performance of phase change material microcapsules with modified carbon nanotubes, Energy 240 (2022) 122821.
[184] R. Chen, X. Huang, R. Zheng, D. Xie, Y. Mei, R. Zou, Flame-retardancy and thermal properties of a novel phosphorus-modified PCM for thermal energy storage, Chemical Engineering Journal 380 (2020) 122500.
[185] M. De Falco, M. Capocelli, G. Losito, V. Piemonte, LCA perspective to assess the environmental impact of a novel PCM-based cold storage unit for the civil air conditioning, Journal of Cleaner Production 165 (2017) 697-704.